RESEARCH ARTICLE SUMMARY

CORONAVIRUS

Immune boosting by B.1.1.529 (Omicron) depends on previous SARS-CoV-2 exposure

Catherine J. Reynolds†, Corinna Pade†, Joseph M. Gibbons†, Ashley D. Otter†, Kai-Min Lin, Diana Muñoz Sandoval, Franziska P. Pieper, David K. Butler, Siyi Liu, George Joy, Nasim Forooghi, Thomas A. Treibel, Charlotte Manisty, James C. Moon, COVIDsortium Investigators§, COVIDsortium Immune Correlates Network§, Amanda Semper, Tim Brooks, Áine McKnight‡, Daniel M. Altmann‡, Rosemary J. Boyton*‡

INTRODUCTION: B.1.1.529 (Omicron) and its subvariants pose new challenges for control of the COVID-19 pandemic. Although vaccinated populations are relatively protected from severe disease and death, countries with high vaccine uptake are experiencing substantial caseloads with breakthrough infection and frequent reinfection.

RATIONALE: We analyzed cross-protective immunity against B.1.1.529 (Omicron) in triple-vaccinated health care workers (HCWs) with different immune-imprinted histories of severe acute respiratory syndrome coronavirus 2 (SARS-CoV-2) infection during the ancestral Wuhan Hu-1, B.1.1.7 (Alpha), and B.1.617.2 (Delta) waves and after infection during the B.1.1.529 (Omicron) wave in previously infection-naïve individuals and those with hybrid immunity, to investigate whether B.1.1.529 (Omicron) infection could further boost adaptive immunity. Spike subunit 1 (S1) receptor binding domain (RBD) and whole spike binding, live virus neutralizing antibody (nAb) potency, memory B cell (MBC) frequency, and T cell responses against peptide pools and naturally processed antigen were assessed.

RESULTS: B and T cell recognition and nAb potency were boosted against previous variants of concern (VOCs) in triple-vaccinated HCWs, but this enhanced immunity was attenuated against B.1.1.529 (Omicron) itself. Furthermore, immune imprinting after B.1.1.7 (Alpha) infection resulted in reduced durability of antibody binding against B.1.1.529 (Omicron), and S1 RBD and whole spike VOC binding correlated poorly with live virus nAb potency. Half of triple-vaccinated HCWs showed no T cell response to B.1.1.529 (Omicron) S1 processed antigen, and all showed reduced responses to the B.1.1.529 (Omicron) peptide pool, irrespective of SARS-CoV-2 infection history. Mapping T cell immunity in class II human leukocyte antigen transgenics showed that individual spike mutations could result in loss or gain of T cell epitope recognition, with changes to T cell effector and regulatory programs. Triple-vaccinated, previously infection-naïve individuals infected during the B.1.1.529 (Omicron) wave showed boosted cross-reactive S1 RBD and whole spike binding, live virus nAb potency, and T cell immunity against previous VOCs but less so against B.1.1.529 (Omicron) itself. Immune imprinting from prior Wuhan Hu-1 infection abrogated any enhanced cross-reactive antibody binding, T cell recognition, MBC frequency, or nAb potency after B.1.1.529 (Omicron) infection.

CONCLUSION: Vaccine boosting results in distinct, imprinted patterns of hybrid immunity with different combinations of SARS-CoV-2 infection and vaccination. Immune protection is boosted by B.1.1.529 (Omicron) infection in the triple-vaccinated, previously infection-naïve individuals, but this boosting is lost with prior Wuhan Hu-1 imprinting. This "hybrid immune damping" indicates substantial subversion of immune recognition and differential modulation through immune imprinting and may be the reason why the B.1.1.529 (Omicron) wave has been characterized by breakthrough infection and frequent reinfection with relatively preserved protection against severe disease in triple-vaccinated individuals. ■

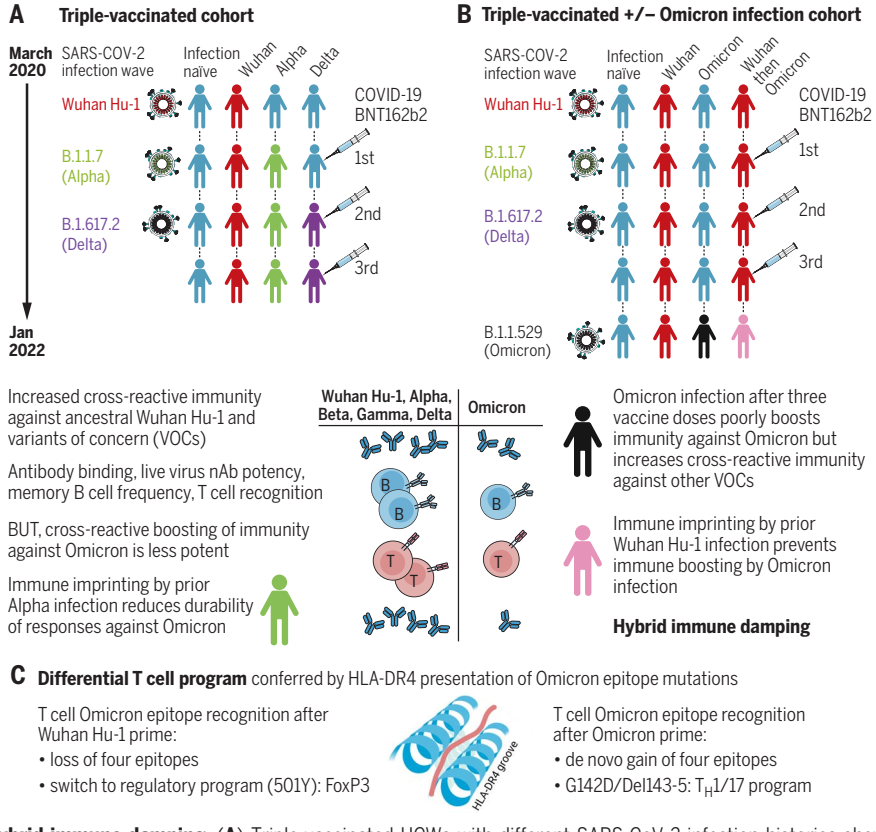

Hybrid immune damping. (**A**) Triple-vaccinated HCWs with different SARS-CoV-2 infection histories show boosted cross-reactive immunity against VOCs, less so against Omicron. (**B**) Breakthrough infection during the Omicron wave boosts cross-reactive immunity in triple-vaccinated, previously infection-naïve individuals against VOCs, less so against Omicron itself; imprinting by previous Wuhan Hu-1 infection ablates Omicron immune boosting. (**C**) T cell recognition of Omicron mutation sequences is linked to altered transcription.

The list of author affiliations is available in the full article online.
*Corresponding author. Email: r.boyton@imperial.ac.uk
†These authors contributed equally to this work.
‡These authors contributed equally to this work.
§The members of the COVIDsortium Investigators and COVIDsortium Immune Correlates Network are listed in the supplementary materials.

Cite this article as C. J. Reynolds *et al.*, *Science* 377, eabq1841 (2022). DOI: 10.1126/science.abq1841

READ THE FULL ARTICLE AT
https://doi.org/10.1126/science.abq1841

RESEARCH ARTICLE

CORONAVIRUS

Immune boosting by B.1.1.529 (Omicron) depends on previous SARS-CoV-2 exposure

Catherine J. Reynolds[1]†, Corinna Pade[2]†, Joseph M. Gibbons[2]†, Ashley D. Otter[3]†, Kai-Min Lin[1], Diana Muñoz Sandoval[1], Franziska P. Pieper[1], David K. Butler[1], Siyi Liu[1], George Joy[4], Nasim Forooghi[4], Thomas A. Treibel[4,5], Charlotte Manisty[4,5], James C. Moon[4,5], COVIDsortium Investigators§, COVIDsortium Immune Correlates Network§, Amanda Semper[3], Tim Brooks[3], Áine McKnight[2]‡, Daniel M. Altmann[6]‡, Rosemary J. Boyton[1,7]*‡

The Omicron, or Pango lineage B.1.1.529, variant of severe acute respiratory syndrome coronavirus 2 (SARS-CoV-2) carries multiple spike mutations with high transmissibility and partial neutralizing antibody (nAb) escape. Vaccinated individuals show protection against severe disease, often attributed to primed cellular immunity. We investigated T and B cell immunity against B.1.1.529 in triple BioNTech BNT162b2 messenger RNA–vaccinated health care workers (HCWs) with different SARS-CoV-2 infection histories. B and T cell immunity against previous variants of concern was enhanced in triple-vaccinated individuals, but the magnitude of T and B cell responses against B.1.1.529 spike protein was reduced. Immune imprinting by infection with the earlier B.1.1.7 (Alpha) variant resulted in less durable binding antibody against B.1.1.529. Previously infection-naïve HCWs who became infected during the B.1.1.529 wave showed enhanced immunity against earlier variants but reduced nAb potency and T cell responses against B.1.1.529 itself. Previous Wuhan Hu-1 infection abrogated T cell recognition and any enhanced cross-reactive neutralizing immunity on infection with B.1.1.529.

At the end of 2021, the severe acute respiratory syndrome coronavirus 2 (SARS-CoV-2) Omicron variant of concern (VOC) spread rapidly, displacing the prior most prevalent VOC, B.1.617.2 (Delta) (*1*, *2*). B.1.1.529 (Omicron) diverges more from the ancestral Wuhan Hu-1 sequence than other VOCs so far, with 36 coding mutations in the spike protein, associated with high transmission, tendency to infect cells of the upper bronchus, and presentation with flu-like symptoms (*3*–*5*). Across several studies, two- or three-dose vaccination is protective against severe disease and hospitalization, albeit with poor protection against transmission (*6*–*8*). A rationale for this high rate of breakthrough infections comes from mapping of virus neutralization using either postvaccination immune sera or monoclonal antibodies, showing Omicron to be the most antibody immune-evasive VOC, with titers generally reduced 20- to 40-fold (*9*–*12*). The relative attenuation of severe symptoms in vaccinated compared with unvaccinated groups is likely attributable to the partial protection conferred by the residual neutralizing antibody (nAb) repertoire and the activation of primed B cell and T cell memory (*13*–*18*). In this study, we applied our ongoing analysis of a cohort of London health care workers (HCWs) (*19*–*24*) to address two key issues of B.1.1.529 (Omicron) immunity. First, following the earlier demonstration that people at this stage in the pandemic carry heterogeneous, immune-imprinted repertoires derived from their distinctive histories of infection and vaccination, we explored how these differences manifest in differential cross-recognition of B.1.1.529 (Omicron) relative to other VOCs, at the level of binding and neutralizing Ab, B cell, and T cell immunity (*24*). Analyzing a London HCW cohort having detailed longitudinal, clinical, transcriptomic, and immunologic characterization, we considered the extent to which prior encounter with spike antigen through infection and vaccination shapes subsequent immunity to B.1.1.529 (Omicron) through immune imprinting. Second, when B.1.1.529 (Omicron) infections and reinfections have been so pervasive (*25*), it is possible that B.1.1.529 (Omicron) infection may confer a benign, live booster to vaccine immunity. Hence, we investigated the extent to which B.1.1.529 (Omicron) infection boosts cross-reactive B and T cell immunity against other VOCs and itself.

[1]Department of Infectious Disease, Imperial College London, London, UK. [2]Blizard Institute, Barts and the London School of Medicine and Dentistry, Queen Mary University of London, London, UK. [3]UK Health Security Agency, Porton Down, UK. [4]St Bartholomew's Hospital, Barts Health NHS Trust, London, UK. [5]Institute of Cardiovascular Science, University College London, London, UK. [6]Department of Immunology and Inflammation, Imperial College London, London, UK. [7]Lung Division, Royal Brompton and Harefield Hospitals, Guy's and St Thomas' NHS Foundation Trust, London, UK.
*Corresponding author. Email: r.boyton@imperial.ac.uk
†These authors contributed equally to this work.
‡These authors contributed equally to this work.
§The members of the COVIDsortium Investigators and COVIDsortium Immune Correlates Network are listed in the supplementary materials.

Results

B cell immunity after three vaccine doses

A London cohort of HCWs were followed longitudinally from March 2020 to January 2022. We identified HCWs with mild and asymptomatic SARS-CoV-2 infection by ancestral Wuhan Hu-1, B.1.1.7 (Alpha VOC), B.1.617.2 (Delta VOC), and then B.1.1.529 (Omicron VOC) during successive waves of infection and after first, second, and third mRNA (BioNTech BNT162b2) vaccine doses (Fig. 1A, fig. S1, and table S1). We identified individuals with different combinations of SARS-CoV-2 infection and vaccination histories to study the impact of immune imprinting. Nucleocapsid (N) and subunit 1 (S1) spike receptor binding domain (RBD) serology was monitored longitudinally (Fig. 1B). As previously reported, the third spike exposure boosted the majority of HCWs above an S1 RBD titer of 1/10,000 binding antibody units per milliliter (U/ml) at 2 to 3 weeks after the most recent vaccine dose. By three vaccine doses, antibody responses had plateaued, regardless of infection history (*24*).

In triple-vaccinated HCWs 2 to 3 weeks after their third dose (table S1), we compared antibody titers against RBD (Fig. 1C), whole spike (fig. S2), and live virus nAb half-maximal inhibitory concentration (IC_{50}) (Fig. 1D) for ancestral Wuhan Hu-1 and each of the VOCs (table S2). We stratified the vaccinated HCWs according to whether they were infection-naïve or had previously been infected with Wuhan Hu-1, B.1.1.7 (Alpha), or B.1.617.2 (Delta) (Fig. 1A). We found differences in immune imprinting indicating that those who were infected during the ancestral Wuhan Hu-1 wave showed a significantly reduced anti-RBD titer against B.1.351 (Beta), P.1 (Gamma), and B.1.1.529 (Omicron) compared with infection-naïve HCWs (Fig. 1C). The hybrid immune groups that had experienced previous Wuhan Hu-1 and B.1.1.7 (Alpha) infection showed more potent nAb responses against Wuhan Hu-1, B.1.1.7 (Alpha), and B.1.617.2 (Delta) (Fig. 1D). However, cross-reactive S1 RBD immunoglobulin G (IgG) antibody and nAb IC_{50} against B.1.1.529 (Omicron) were significantly reduced compared with the other VOCs, irrespective of previous SARS-CoV-2 infection history (table S3 and Fig. 1, C and D).

Memory B cell (MBC) frequencies against ancestral Wuhan Hu-1, B.1.617.2 (Delta), and B.1.1.529 (Omicron) S1 protein were boosted 2 to 3 weeks after the third vaccine dose compared with 20 to 21 weeks after the second vaccine dose (Fig. 1E). Irrespective of infection history, the MBC frequencies against Wuhan Hu-1 and B.1.617.2 (Delta) S1 were similar, but those against B.1.1.529 (Omicron) S1 were significantly reduced 2 to 3 weeks after the third vaccine dose [reduction in B.1.1.529 (Omicron) S1 MBC frequency compared with Wuhan Hu-1 S1 was 2.0-fold (P = 0.0156) for infection-naïve, 2.4-fold for Wuhan Hu-1 infection (P = 0.0020),

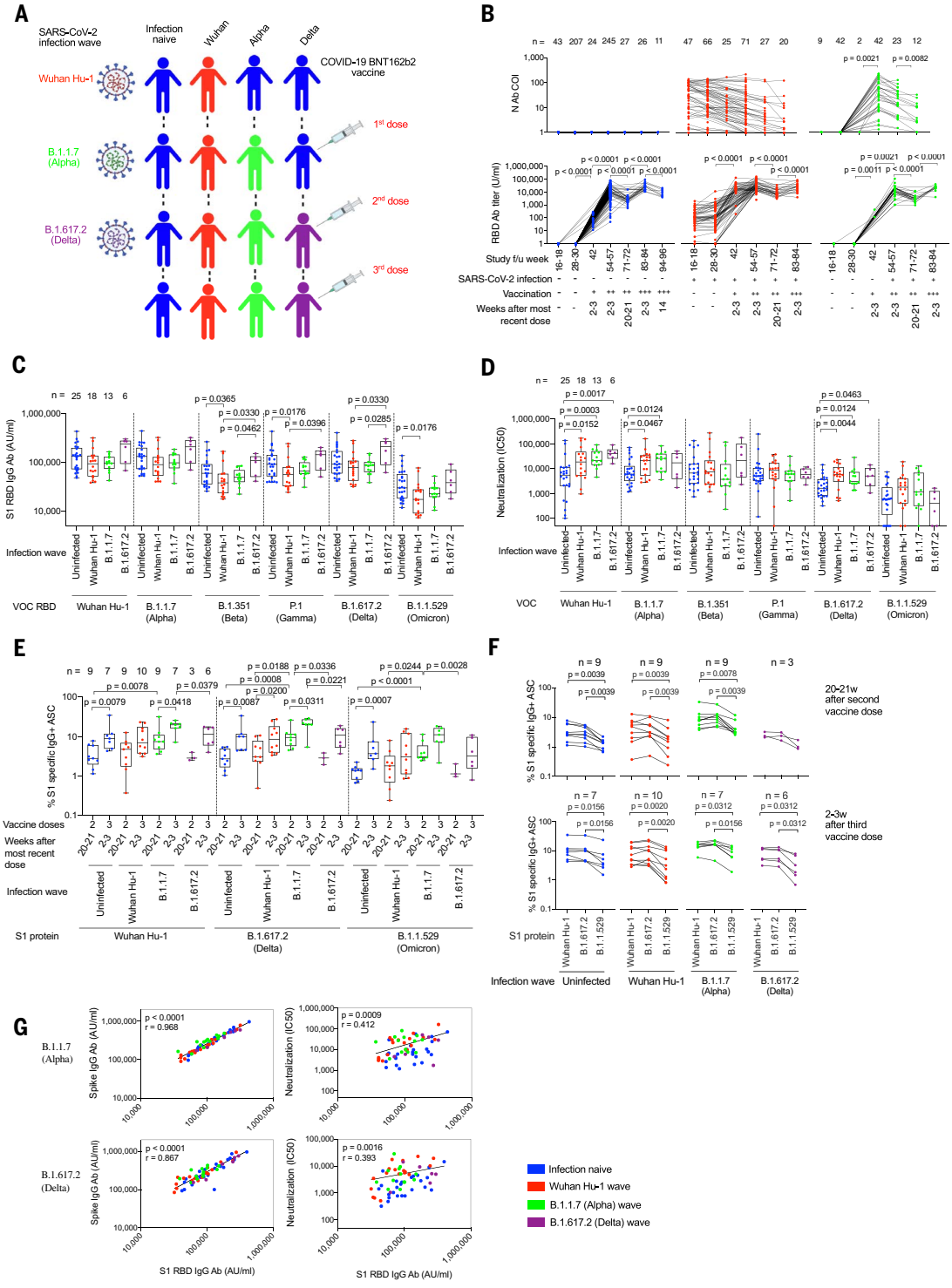

Fig. 1. SARS-CoV-2 infection history alters Ab and B cell immunity in triple-vaccinated HCWs. (**A**) Graphical summary depicting the SARS-CoV-2 infection and vaccination history of HCWs studied. (**B**) Serum Ab binding against SARS-CoV-2 N (top panel) and ancestral Wuhan Hu-1 S1 RBD (bottom panel) in infection-naïve HCWs (blue, n = 11 to 245) and HCWs with laboratory-confirmed SARS-CoV-2 infection during the Wuhan Hu-1 (red, n = 20 to 71) or B.1.1.7 (Alpha, green, n = 12 to 42) waves. Data are shown pre-vaccination and at defined time points after a first, second, and third dose of BNT162b2. (**C**) Serum S1 RBD Ab binding and (**D**) nAb IC_{50} against ancestral Wuhan Hu-1, B.1.1.7 (Alpha), B.1.351 (Beta), P.1 (Gamma), B.1.617.2 (Delta), and B.1.1.529 (Omicron) live virus 2 to 3 weeks after the third vaccine dose in infection-naïve HCWs (blue, n = 25) or HCWs with laboratory-confirmed SARS-CoV-2 infection during the ancestral Wuhan Hu-1 (red, n = 18), B.1.1.7 (Alpha, green, n = 13), or B.1.617.2 (Delta, purple, n = 6) waves. (**E**) Frequency of MBC specific for ancestral Wuhan Hu-1, B.1.617.2 (Delta), and B.1.1.529 (Omicron) spike S1 protein 20 to 21 weeks after the second and 2 to 3 weeks after the third vaccine dose in infection-naïve (blue, n = 7 to 9) or HCWs infected by SARS-CoV-2 during the Wuhan Hu-1 (red, n = 9 to 10), B.1.1.7 (Alpha, green, n = 7 to 9), or B.1.617.2 (Delta, purple, n = 3 to 6) waves. (**F**) MBC frequency data plotted pairwise for individual HCWs at 20 to 21 weeks after second dose (top panel) or 2 to 3 weeks after third dose (bottom panel). (**G**) Correlations between S1 RBD VOC and whole spike VOC Ab binding (left-hand panel) and nAb IC_{50} (right-hand panel) against B.1.1.7 (Alpha) and B.1.617.2 (Delta) in infection-naïve (blue, n = 25) HCWs and HCWs infected during the ancestral Wuhan Hu-1 (red, n = 18), B.1.1.7 (Alpha, green, n = 13), and B.1.617.2 (Delta, purple, n = 6) waves. Statistical tests were performed using Prism 9.0. [(B) to (E)] Mann-Whitney U test, (F) Wilcoxon matched-pairs signed rank test, (G) Spearman's rank correlation. f/u; follow-up; w, weeks.

1.9-fold for B.1.1.7 (Alpha) infection (P = 0.0312), and 2.9-fold for B.1.617.2 (Delta) infection (P = 0.0312)] and at 20 to 21 weeks after the second dose [reduction in B.1.1.529 (Omicron) MBC frequency compared with Wuhan Hu-1 was 2.5-fold (P = 0.0039) for infection-naïve HCWs and 2.2-fold (P = 0.0039), twofold (P = 0.0078), and 2.9-fold (P = 0.1250) for Wuhan Hu-1, B.1.1.7 (Alpha), and B.1.617.2 (Delta) infection groups, respectively] (Fig. 1F and table S4).

S1 RBD or whole spike antibody binding and live virus nAb IC_{50} correlated for B.1.1.7 (Alpha) and B.1.617.2 (Delta), but not for B.1.351 (Beta), P.1 (Gamma), or B.1.1.529 (Omicron), indicating that antibody binding serology was a poor marker of nAb IC_{50} (Fig. 1G and fig. S3). Differences between VOC RBD and whole spike binding and nAb IC_{50} with live virus indicated

that antibody targeting regions outside RBD and/or spike or conformational epitopes exposed only during infection may contribute to neutralization (*26*, *27*) (Fig. 1, C and D).

T cell immunity after three vaccine doses

We next compared T cell responses at 2 to 3 weeks after the third dose in triple-vaccinated HCWs who were either infection-naïve or had been infected during the Wuhan Hu-1, B.1.1.7 (Alpha), or B.1.617.2 (Delta) wave (fig. S1 and table S1). We compared T cell immunity against a mapped epitope pool (MEP) of ancestral Wuhan Hu-1 spike peptides (table S5A) with spike S1 protein from ancestral Wuhan Hu-1 or S1 proteins containing the B.1.617.2 (Delta) or B.1.1.529 (Omicron) mutations. Measuring T cell responses against naturally processed epitopes from whole S1 protein antigen of ancestral Wuhan Hu-1, B.1.617.2 (Delta), or B.1.1.529 (Omicron) sequence allowed us to focus on immunodominant responses representative of those presented in real-life infection. T cell responses against Wuhan Hu-1 S1 protein mirrored those elicited by MEP stimulation, with the majority making a strong response (Fig. 2A). However, for S1 B.1.1.529 (Omicron) protein, we found a significantly reduced magnitude of response. Overall, more than half (27/50, 54%) made no T cell response against S1 B.1.1.529 (Omicron) protein, irrespective of previous SARS-CoV-2 infection history, compared with 8% (4/50) that made no T cell response against ancestral Wuhan Hu-1 S1 protein ($P < 0.0001$, Chi-square test) (Fig. 2A). The fold-reduction in geometric mean of T cell response [spot forming cells (SFCs)] against B.1.1.529 (Omicron) S1 compared with ancestral Wuhan Hu-1 S1 protein was 17.3-fold for infection-naïve HCWs (blue, $P < 0.0001$), 7.7-fold for previously Wuhan Hu-1 infected (red, $P = 0.001$), 8.5-fold for previously B.1.1.7 (Alpha) infected (green, $P = 0.002$), and 19-fold for previously B.1.617.2 (Delta) infected (purple, $P = 0.0625$) HCWs (Fig. 2B).

To investigate T cell recognition of VOC sequence mutations, we used a peptide pool specifically designed to cover all of the B.1.1.529 (Omicron) S1 and S2 spike mutations and a matched pool containing the equivalent Wuhan Hu-1 sequences (Fig. 2C and table S5B). T cell responses against the B.1.1.529 (Omicron) peptide pool were reduced compared with the Wuhan Hu-1 pool, irrespective of previous infection history [reduction in T cell response against B.1.1.529 (Omicron) peptide pool compared with equivalent ancestral Wuhan Hu-1 peptide pool was 2.7-fold for infection-naïve (blue, $P = 0.0003$), 4.6-fold for previously Wuhan Hu-1 infected (red, $P = 0.0039$), 2.7-fold for previously B.1.1.7 (Alpha) infected (green, $P = 0.0039$), and 3.8-fold for previously B.1617.2 (Delta) infected HCWs (purple, $P = 0.1250$)] (Fig. 2C). In fact, 42% (21/50) of HCWs made no T cell response at all against the B.1.1.529 (Omicron) VOC mutant pool (Fig. 2C).

Overall, our findings in triple-vaccinated HCWs with different previous SARS-CoV-2 infection histories indicated that T cell cross-recognition of B.1.1.529 (Omicron) S1 antigen and peptide pool was significantly reduced. T cell and nAb responses against B.1.1.529

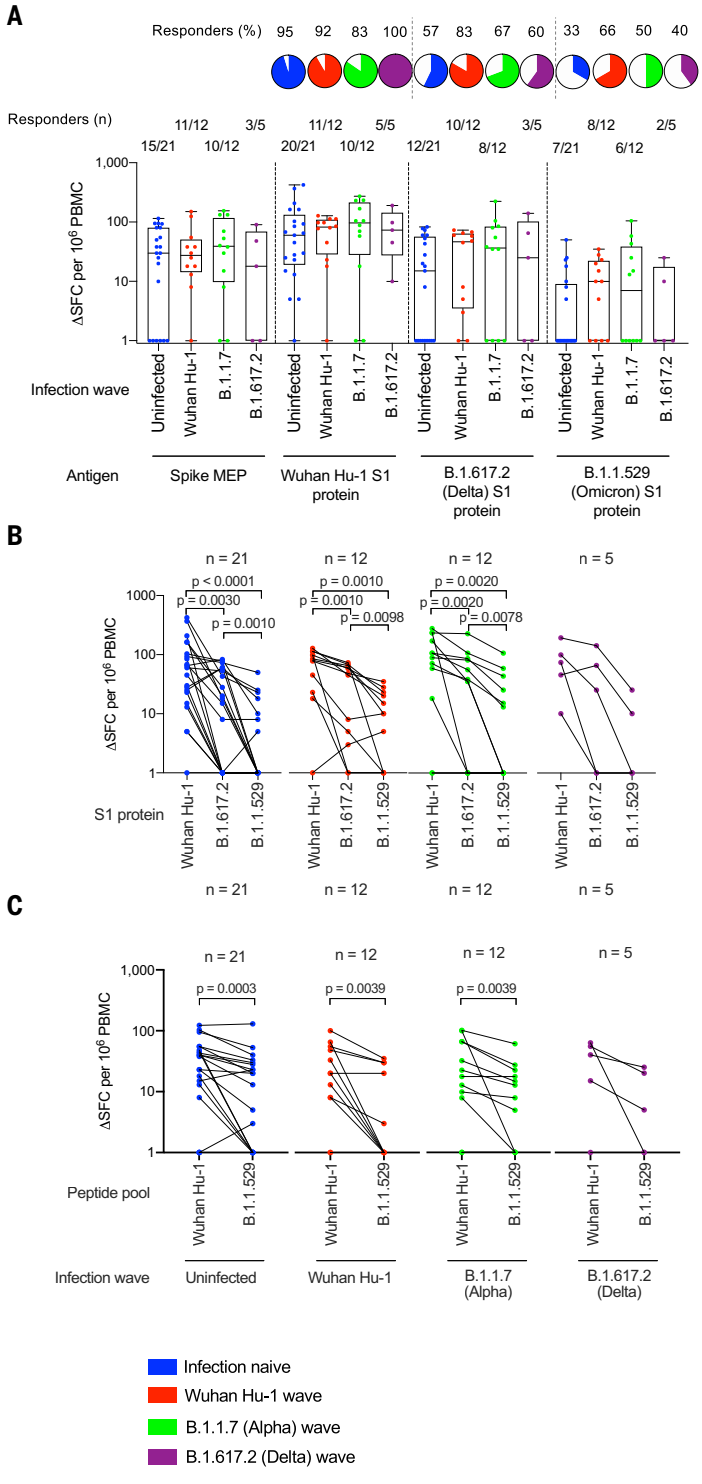

Fig. 2. T cell cross-recognition of B.1.1.529 (Omicron) in triple-vaccinated HCWs. (**A**) T cell responses against ancestral Wuhan Hu-1 spike MEP pool or ancestral Wuhan Hu-1, B.1.617.2 (Delta), and B.1.1.529 (Omicron) VOC S1 proteins in PBMC from infection-naïve HCWs (blue) or HCWs with laboratory-confirmed SARS-CoV-2 infection during the ancestral Wuhan Hu-1 (red), B.1.1.7 (Alpha, green), and B.1.617.2 (Delta, purple) waves. PBMCs were taken 2 to 3 weeks after the third vaccine dose, and T cell responses assessed by IFNγ ELISpot. Pie charts show the percent of responders with a detectable T cell response against each antigen. (**B**) Spike MEP pool and S1 protein T cell responses plotted pair-wise for each individual HCW. (**C**) T cell responses against peptide pools containing either the B.1.1.529 (Omicron) mutations found in the SARS-CoV-2 spike or the equivalent original ancestral Wuhan Hu-1 sequences. PBMCs from infection-naïve HCWs (blue) or HCWs infected during the ancestral Wuhan Hu-1 (red), B.1.1.7 (Alpha, green), or B.1.617.2 (Delta, purple) waves were stimulated by peptide pools containing the original Wuhan Hu-1 or B.1.1.529 sequences and plotted pair-wise. Statistical tests were performed using Prism 9.0. (A) Mann-Whitney *U* test, [(B) and (C)] Wilcoxon matched-pairs signed rank test.

(Omicron) were discordant, and most (20/27, 74%) HCWs with no T cell response against B.1.1.529 (Omicron) S1 made cross-reactive nAb against B.1.1.529 at an IC_{50} of >195 (fig. S4).

B.1.1.529 (Omicron) spike mutations encompass gain and loss of T cell epitopes

Owing to the complexities inherent in mapping the effects of mutations in individual T cell epitopes across cohorts carrying heterogeneous human leukocyte antigen (HLA) alleles, we mapped the differential recognition of the B.1.1.529 (Omicron) spike mutations using HLA-DRB1*04:01 transgenic mice (*23*, *24*) (Fig. 3). The peptide pool containing B.1.1.529

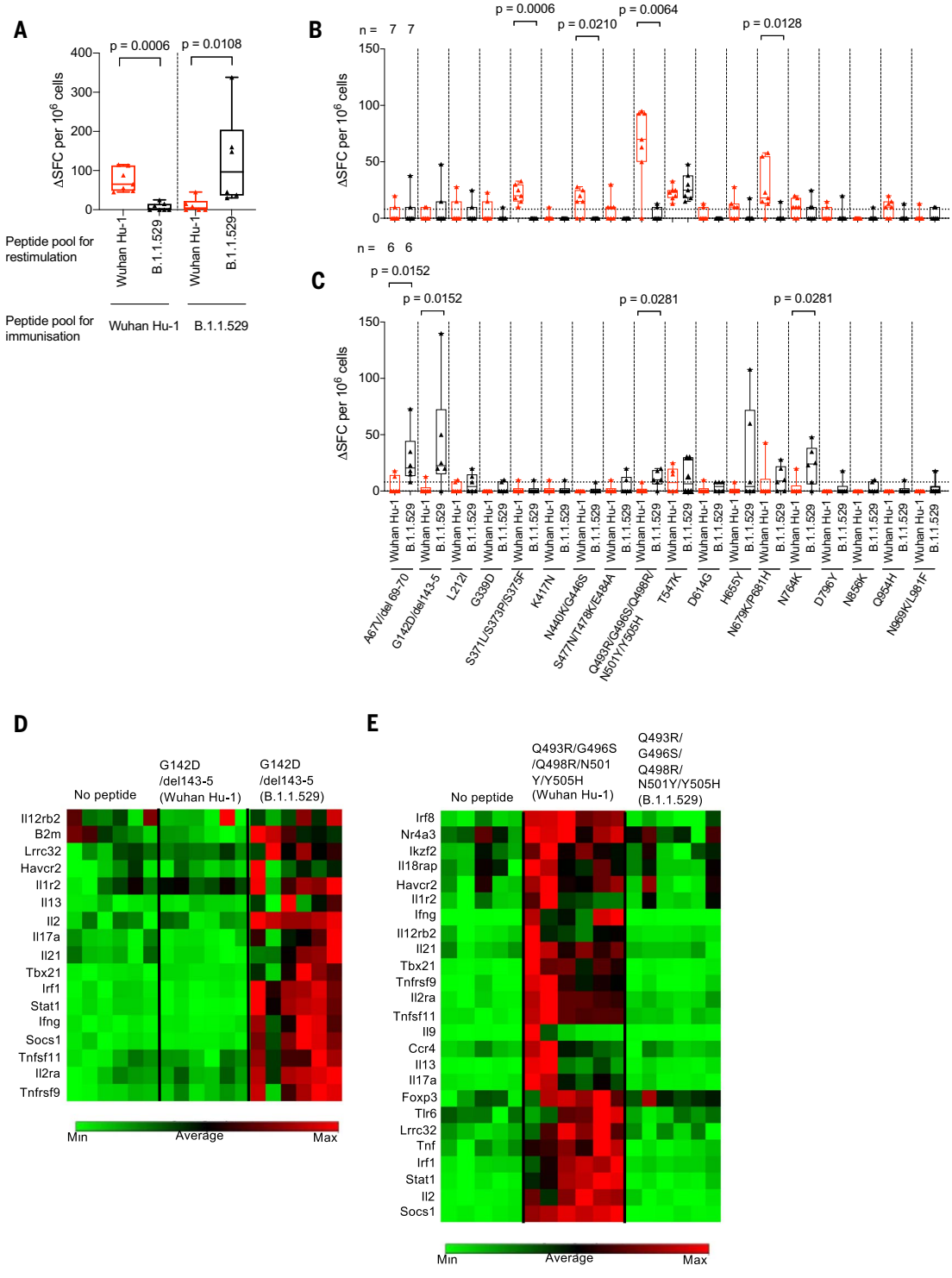

Fig. 3. B.1.1.529 (Omicron) spike mutations alter T cell recognition. (**A**) HLAII transgenic mice carrying DRB1*0401 in the context of a homozygous knockout for murine H2-Aβ (7 to 8 weeks old) were immunized with either a B.1.1.529 (Omicron, *n* = 7) VOC pool of 18 peptides encompassing the Omicron sequence mutations or the ancestral Wuhan Hu-1 pool of peptides (*n* = 6) with the equivalent unmutated sequences. At day 10, draining lymph node (DLN) cells were prepared from immunized mice and stimulated with either Wuhan Hu-1 (red) or B.1.1.529 (Omicron, black) peptide pools, and T cell responses were measured by IFNγ ELISpot. (**B**) IFNγ T cell responses were mapped against individual Wuhan Hu-1 (red) or B.1.1.529 (Omicron, black) peptides using DLN cells taken from Wuhan Hu-1 peptide pool (*n* = 7) or (**C**) B.1.1.529 (Omicron) peptide pool (*n* = 6) immunized mice. Single-letter abbreviations for the amino acid residues are as follows: A, Ala; C, Cys; D, Asp; E, Glu; F, Phe; G, Gly; H, His; I, Ile; K, Lys; L, Leu; M, Met; N, Asn; P, Pro; Q, Gln; R, Arg; S, Ser; T, Thr; V, Val; W, Trp; and Y, Tyr. (**D** and **E**) Heatmaps showing relative gene expression of T cell activation markers in DLN cells taken from B.1.1.529 (Omicron) G142D/del143-5 peptide primed (D) (*n* = 6) or Wuhan Hu-1 Q493R/G496S/Q498R/N501Y/Y505H peptide primed (E) (*n* = 6) HLA-DRB1*04:01 transgenic mice. DLN cells were stimulated for 24 hours in vitro with 10 μg/ml Wuhan Hu-1 or B.1.1.529 (Omicron) variant peptide before RNA extraction. Genes shown in the heatmap are significantly up-regulated ($P < 0.05$) in Wuhan Hu-1 or B.1.1.529 (Omicron) variant peptide stimulated cells compared with no peptide control. Statistical tests were performed using Prism 9.0 or the Qiagen GeneGlobe data analysis tool for gene expression data. [(A) to (C)] Wilcoxon matched-pairs signed rank test, [(D) and (E)] Student's *t* test.

(Omicron)–specific S1 and S2 spike mutations and its ancestral Wuhan Hu-1 equivalent pool showed differential, sequence-specific T cell priming by either ancestral Wuhan Hu-1 or B.1.1.529 (Omicron) sequence-specific peptide pools (Fig. 3A and table S5B). That is, immunizing HLAII transgenic mice with either ancestral Wuhan Hu-1 or B.1.1.529 (Omicron) sequence-specific peptide pools allowed us to investigate differential, sequence-specific T cell priming that occurs as a consequence of B.1.1.529 (Omicron) spike mutations. We showed that priming with one pool resulted in impaired responses to the other (Fig. 3A). We then looked at responses to individual HLA-DRB1*04:01 epitopes. Notably, while the B.1.1.529 (Omicron) mutations were associated in four instances with loss of a clear HLA-DR4–restricted T cell epitope (Fig. 3B: S371L/S373P/S375F, $P = 0.0006$; N440K/G446S, $P = 0.0210$; Q493R/G496S/Q498R/N501Y/Y505H, $P = 0.0064$; N679K/P681H, $P = 0.0128$), the mutated sequence epitopes in four instances led to de novo gain of Omicron-specific HLA-DR4 T cell epitopes (Fig. 3C: A67V/del69-70, $P = 0.0152$; G142D/del143-5, $P = 0.0152$; Q493R/G496S/Q498R/N501Y/Y505H/N679K/P681H, $P = 0.0281$; N764K, $P = 0.0281$). The G142D/del143-5 mutation created a gain-of-function epitope, switching from a region not recognized by T cells to one that induced a T helper 1 (T_H1)/T_H17 effector program (Fig. 3D). We have previously shown that the N501Y mutation converts a T cell effector–stimulating epitope to an inducer of immune regulation (*24*). This finding was confirmed and reiterated by the more extensive alterations in the Q493R/G496S/Q498R/N501Y/Y505H mutant epitope (Fig. 3E).

B cell immunity after B.1.1.529 (Omicron) infection

Next, we studied triple-vaccinated HCWs 14 weeks after their third dose, who had suffered breakthrough infection during the B.1.1.529 (Omicron) wave. These individuals were compared with infection-naïve and previously Wuhan Hu-1 infected HCWs who had escaped B.1.1.529 (Omicron) wave infection (Fig. 4A, tables S6 and S7, and fig. S1). Previously Wuhan Hu-1 infected HCWs who were also infected during the B.1.1.529 (Omicron) wave showed the highest N antibody binding (Fig. 4B and tables S6 and S7). Previously infection-naïve triple-vaccinated HCWs made significantly increased cross-reactive antibody binding responses against all VOCs and B.1.1.529 (Omicron) itself after infection during the B.1.1.5129 (Omicron) wave: S1 RBD (Fig. 4C and table S2), whole spike (Fig. 4D and table S2), and nAb IC_{50} (Fig. 4E). However, antibody binding and nAb IC_{50} were attenuated against B.1.1.529 (Omicron) itself with a 4.5-fold reduction in S1 RBD binding ($P = 0.001$) and a 10.1-fold reduction in nAb IC_{50} ($P = 0.002$) against B.1.1.529 compared with ancestral Wuhan Hu-1. Thus, infection during the B.1.1.529 (Omicron) wave produced potent cross-reactive antibody immunity against all VOCs, but less so against B.1.1.529 (Omicron) itself.

Triple-vaccinated, infection-naïve HCWs who were not infected during the B.1.1.529 (Omicron) wave made no nAb IC_{50} response against B.1.1.529 (Omicron) 14 weeks after the third vaccine dose, indicating rapid waning of the nAb IC_{50} from a mean value of 1400 at 2 to 3 weeks to 0 at 14 weeks after the third dose ($P = 0.0312$) (Fig. 4E and fig. S5A).

HCWs with a history of prior Wuhan Hu-1 infection who were also infected during the B.1.1.529 (Omicron) wave showed no increase in cross-reactive S1 RBD (Fig. 4C) or whole spike (Fig. 4D) antibody binding or live virus nAb IC_{50} (Fig. 4E and fig. S5B) against B.1.1.529 (Omicron) or any other VOC, despite having made a higher N antibody response (Fig. 4B). Thus, B.1.1.529 (Omicron) infection can boost binding and nAb responses against itself and other VOCs in triple-vaccinated previously uninfected infection-naïve HCWs but not in the context of immune imprinting after prior Wuhan Hu-1 infection. Immune imprinting by prior Wuhan Hu-1 infection completely abrogated any enhanced nAb responses against B.1.1.529 (Omicron) and other VOCs (Fig. 4E).

Increased MBC frequency against ancestral Wuhan Hu-1, B.1.617.2 (Delta), and B.1.1.529 (Omicron) S1 and RBD proteins was observed in previously infection-naïve HCWs infected during the B.1.1.529 (Omicron) wave (Fig. 4F). This was not the case for HCWs who had been previously infected during the first Wuhan Hu-1 wave and then infected again during the B.1.1.529 (Omicron) wave (Fig. 4F).

In summary, B.1.1.529 (Omicron) infection resulted in enhanced, cross-reactive Ab responses against all VOCs tested in the three-dose vaccinated infection-naïve HCWs but not in those with previous Wuhan Hu-1 infection, and less so against B.1.1.529 (Omicron) itself (Fig. 4, C to E). In line with this, MBC frequencies against Wuhan Hu-1, B.1.617.2 (Delta), and B.1.1.529 (Omicron) S1 and RBD proteins increased in three-dose vaccinated, infection-naïve individuals but not in those imprinted by previous Wuhan Hu-1 infection (Fig. 4F).

S1 RBD or whole spike antibody binding and live virus nAb IC_{50} correlated for B.1.1.529 (Omicron) [correlation coefficient (r) of 0.687, $P < 0.0001$] and all the VOCs tested ($r > 0.539$), but there was considerable discordance in that many of the HCWs recording no detectable live virus nAb IC_{50} against B.1.1.529 (Omicron) recorded S1 RBD (Omicron) binding serology ranging from 3412 to 20,484, indicating that S1 RBD (VOC) antibody binding serology could be misleading and a poor marker of nAb (Fig. 4G and fig. S6).

T cell immunity after B.1.1.529 (Omicron) infection

We next explored T cell immunity after breakthrough infection during the B.1.1.529 (Omicron) wave. Fourteen weeks after the third dose (9/10, 90%) of triple-vaccinated, previously infection-naïve HCWs showed no cross-reactive T cell immunity against B.1.1.529 (Omicron) S1 protein (Fig. 5A).

The T cell response against B.1.1.529 (Omicron) S1 protein after infection during the B.1.1.529 (Omicron) wave of previously infection-naïve HCWs was significantly reduced compared with Wuhan Hu-1 S1 and B.1.617.2 (Delta) S1 in triple-vaccinated HCWs [geometric mean: 57, 50, and 6 SFCs for Wuhan Hu-1, B.1.617.2 (Delta), and B.1.1.529 (Omicron) S1 proteins, respectively; $P = 0.001$)] (Fig. 5B). HCWs infected during the B.1.1.529 (Omicron) wave showed similar T cell responses against spike MEP, ancestral Wuhan Hu-1 S1, and B.1.617.2 (Delta) S1 proteins but significantly reduced T cell responses against B.1.1.529 (Omicron) S1 protein [reduction in geometric mean of T cell response (SFCs) against VOC S1 protein compared with that for Wuhan Hu-1 S1: 1.1-fold reduction for B.1.617.2 S1, $P = 0.6836$; 10-fold reduction for B.1.1.529 S1, $P = 0.001$] (Fig. 5B). Thus, although breakthrough infection in triple-vaccinated HCWs during the Omicron infection wave boosted cross-reactive T cell immune recognition against the spike MEP pool ($P = 0.0117$), ancestral Wuhan Hu-1 ($P = 0.0039$), B.1.617.2 (Delta) ($P = 0.0003$), and B.1.1.529 (Omicron) (Fig. 5A), the T cell response against B.1.1.529 (Omicron) S1 protein itself compared with spike MEP ($P = 0.001$), Wuhan Hu-1 ($P = 0.001$), and B.1.617.2 (Delta) ($P = 0.001$) was significantly reduced (Fig. 5, B and C).

Notably, none (0/6) of HCWs with a previous history of SARS-CoV-2 infection during the Wuhan Hu-1 wave responded to B.1.1.529 (Omicron) S1 protein (Fig. 5A). This suggests that, in this context, B.1.1.529 (Omicron) infection was unable to boost T cell immunity against B.1.1.529 (Omicron) itself; immune imprinting from prior Wuhan Hu-1 infection resulted in the absence of a T cell response against B.1.1.529 (Omicron) S1 protein. These findings were further highlighted in paired data showing the fall in T cell response in individual HCWs across the three antigens: On an individual basis, most HCWs retained T cell recognition of B.1.617.2 S1 but commonly showed impaired T cell recognition of B.1.1.529 S1 (Fig. 5C). Taken together with the data shown in Fig. 4, the findings consistently demonstrate that people initially infected by Wuhan Hu-1 in the first wave and then reinfected during the B.1.1.529 (Omicron) wave do not experience a boost in T cell immunity against B.1.1.529 (Omicron) at the level of nAb and T cell recognition.

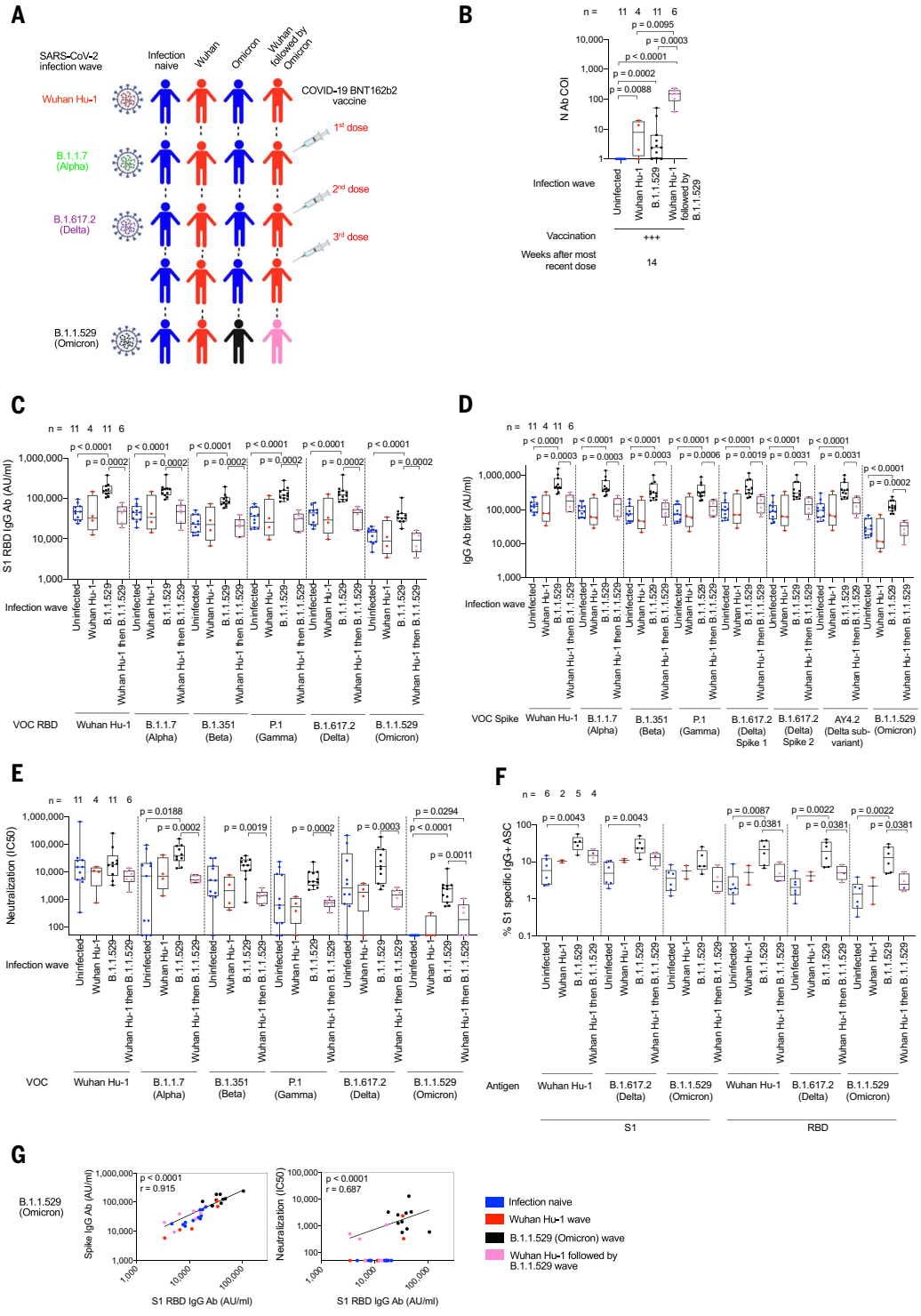

Fig. 4. Ab and B cell immunity in triple-vaccinated HCWs after infection during the B.1.1.529 (Omicron) wave. (**A**) Graphical summary depicting the SARS-CoV-2 infection and vaccination history of HCWs studied during the B.1.1.529 (Omicron) wave. (**B**) Serum Ab binding against SARS-CoV-2 N at 14 weeks (median, 14 weeks; IQR, 3 weeks) after third vaccine dose in infection-naïve HCWs (blue, *n* = 11) or in HCWs with laboratory-confirmed SARS-CoV-2 infection during the ancestral Wuhan Hu-1 (red, *n* = 4), B.1.1.529 (Omicron, black, *n* = 11), or Wuhan Hu-1 followed by B.1.1.529 (Omicron, pink, *n* = 6) infection waves. (**C**) Serum S1 RBD (VOC) Ab binding against ancestral Wuhan Hu-1, B.1.1.7 (Alpha), B.1.351 (Beta), P.1 (Gamma), B.1.617.2 (Delta), and B.1.1.529 (Omicron) proteins in infection-naïve HCWs (blue, *n* = 11) or HCWs previously infected during the ancestral Wuhan Hu-1 (red, *n* = 4), B.1.1.529 (Omicron, black, *n* = 11), or Wuhan Hu-1 followed by B.1.1.529 (Omicron, pink, *n* = 6) waves. (**D**) Serum Ab binding against ancestral Wuhan Hu-1, B.1.1.7 (Alpha), B.1.351 (Beta), P.1 (Gamma), B.1.617.2 (Delta), AY4.2 (Delta subvariant), and B.1.1.529 (Omicron) whole spike proteins in infection-naïve HCWs (blue, *n* = 11) or HCWs previously infected during the ancestral Wuhan Hu-1 (red, *n* = 4), B.1.1.529 (Omicron, black, *n* = 11), or Wuhan Hu-1 followed by B.1.1.529 (Omicron, pink, *n* = 6) waves. (**E**) Neutralizing antibody IC_{50} against Wuhan Hu-1 or VOC live virus isolates in infection-naïve HCWs (blue, *n* = 11) or HCWs previously infected during the ancestral Wuhan Hu-1 (red, *n* = 4), B.1.1.529 (Omicron, black, *n* = 11), or Wuhan Hu-1 followed by B.1.1.529 (Omicron, pink, *n* = 6) waves. (**F**) Frequency of MBC specific for ancestral Wuhan Hu-1, B.1.617.2 (Delta), and B.1.1.529 (Omicron) S1 and RBD binding proteins in infection-naïve HCWs (blue, *n* = 11) or HCWs previously infected during the ancestral Wuhan Hu-1 (red, *n* = 4), B.1.1.529 (Omicron, black, *n* = 11), or Wuhan Hu-1 followed by B.1.1.529 (Omicron, pink, *n* = 6) waves. (**G**) Correlation between whole spike and S1 RBD Ab binding (left-hand panel) or nAb IC_{50} and S1 RBD Ab binding (right-hand panel) for B.1.1.529 (Omicron) VOC in infection-naïve (blue, *n* = 11) or HCWs infected during the ancestral Wuhan Hu-1 (red, *n* = 4), B.1.1.529 (Omicron, black, *n* = 11), or Wuhan Hu-1 followed by B.1.1.529 (Omicron, pink, *n* = 6) waves. All data shown are from samples taken at 14 weeks (median, 14 weeks; IQR, 3 weeks) after third vaccine dose. Statistical tests were performed using Prism 9.0. [(B) to (F)] Mann-Whitney *U* test, (G) Spearman's rank correlation.

Prior infection differentially imprints Omicron T and B cell immunity

To investigate in more detail the impact of prior SARS-CoV-2 infection on immune imprinting, we further explored responses in our longitudinal HCW cohort (Fig. 6A and fig. S1). We first looked at the S1 RBD (ancestral Wuhan Hu-1 and Omicron VOC) antibody binding responses across the longitudinal cohort at key vaccination and SARS-CoV-2 infection time points, exploring how different exposure imprinted differential cross-reactive immunity and durability. This revealed that at 16 to 18 weeks after Wuhan Hu-1 or B.1.1.7 (Alpha) infection, unvaccinated HCWs showed no detectable

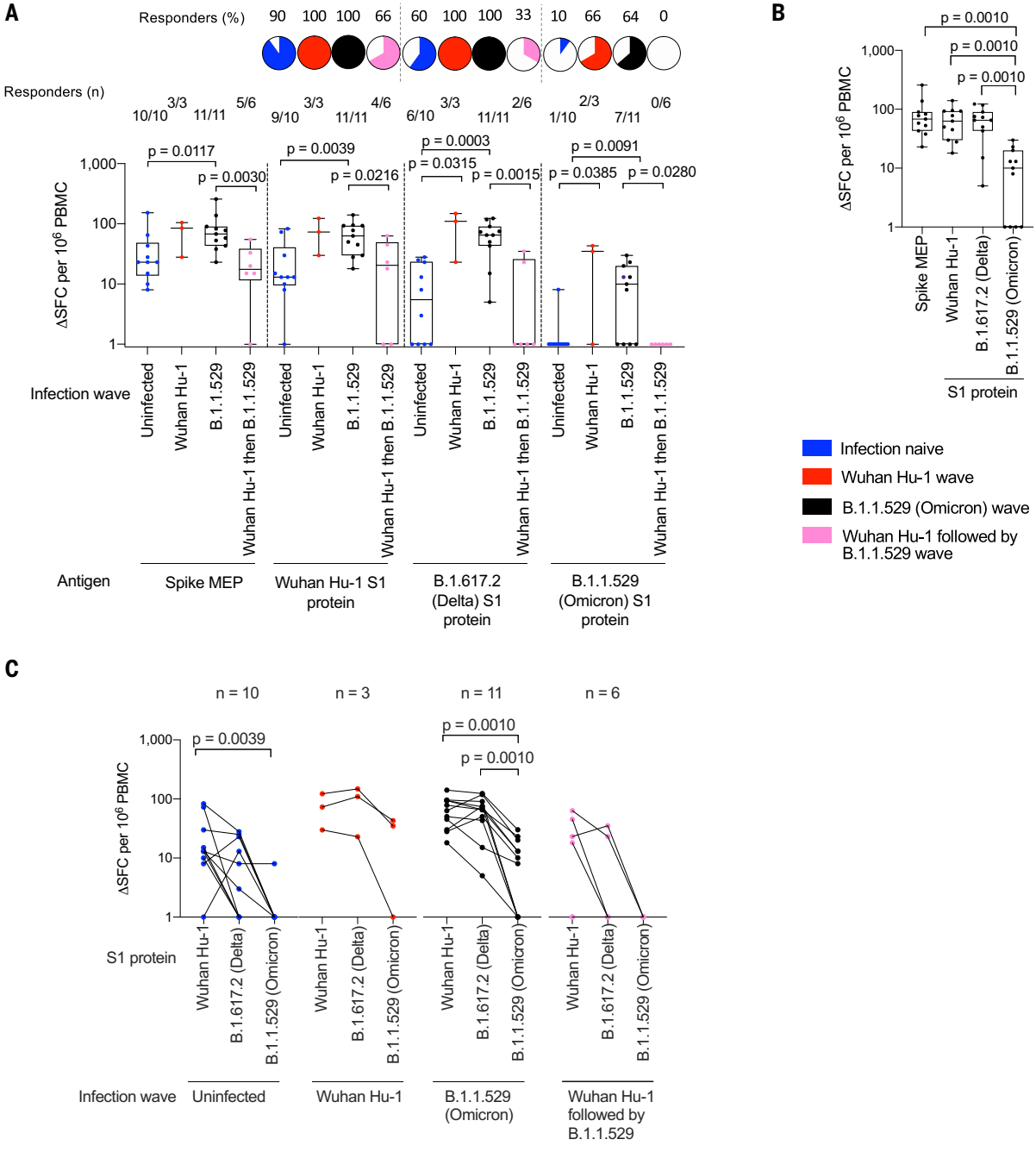

Fig. 5. T cell responses in triple-vaccinated HCWs infected during the B.1.1.529 (Omicron) wave. (**A**) T cell responses against ancestral Wuhan Hu-1 spike MEP pool or Wuhan Hu-1, B.1.617.2 (Delta), and B.1.1.529 (Omicron) VOC S1 protein for PBMCs taken from infection-naïve HCWs (blue, *n* = 10) or HCWs with laboratory-confirmed SARS-CoV-2 infection during the Wuhan Hu-1 (red, *n* = 3), B.1.1.529 (Omicron, black, *n* = 11), or Wuhan Hu-1 followed by B.1.1.529 (Omicron, pink, *n* = 6) waves. PBMCs were taken 14 weeks (median, 14 weeks; IQR, 3 weeks) after the third vaccine dose, and T cell responses were assessed by IFNγ ELISpot. Pie charts show the percent who had a detectable T cell response against each antigen. (**B**) T cell responses against spike MEP pool and S1 VOC protein for previously infection-naïve triple-vaccinated HCWs infected during the B.1.1.529 (Omicron, black, *n* = 11) wave. (**C**) T cell responses against ancestral Wuhan Hu-1, B.1.617.2 (Delta), and B.1.1.529 (Omicron) S1 proteins plotted pair-wise for infection-naïve HCWs (blue, *n* = 10) or HCWs with laboratory-confirmed SARS-CoV-2 infection during the Wuhan Hu-1 (red, *n* = 3), B.1.1.529 (Omicron, black, *n* = 11), or Wuhan Hu-1 followed by B.1.1.529 (Omicron, pink, *n* = 6) waves. Statistical tests were performed using Prism 9.0. (A) Mann-Whitney *U* test, [(B) and (C)] Wilcoxon matched-pairs signed rank test.

cross-reactive S1 RBD binding antibodies against B.1.1.529 (Omicron) (Fig. 6C).

Hybrid immunity (the combination of prior infection and a single vaccine dose) significantly increased the S1 RBD binding antibodies against B.1.1.529 (Omicron) ($P < 0.0001$) compared with responses of infection-naïve HCWs, which were undetectable after a single vaccine dose. This increase was significantly greater for previously Wuhan Hu-1 infected than B.1.1.7 (Alpha) infected HCWs ($P < 0.0002$) (Fig. 6, B and C).

At 2 to 3 weeks after two vaccine doses, there was a leveling up of S1 RBD B.1.1.529 (Omicron) binding antibody, such that infection-naïve,

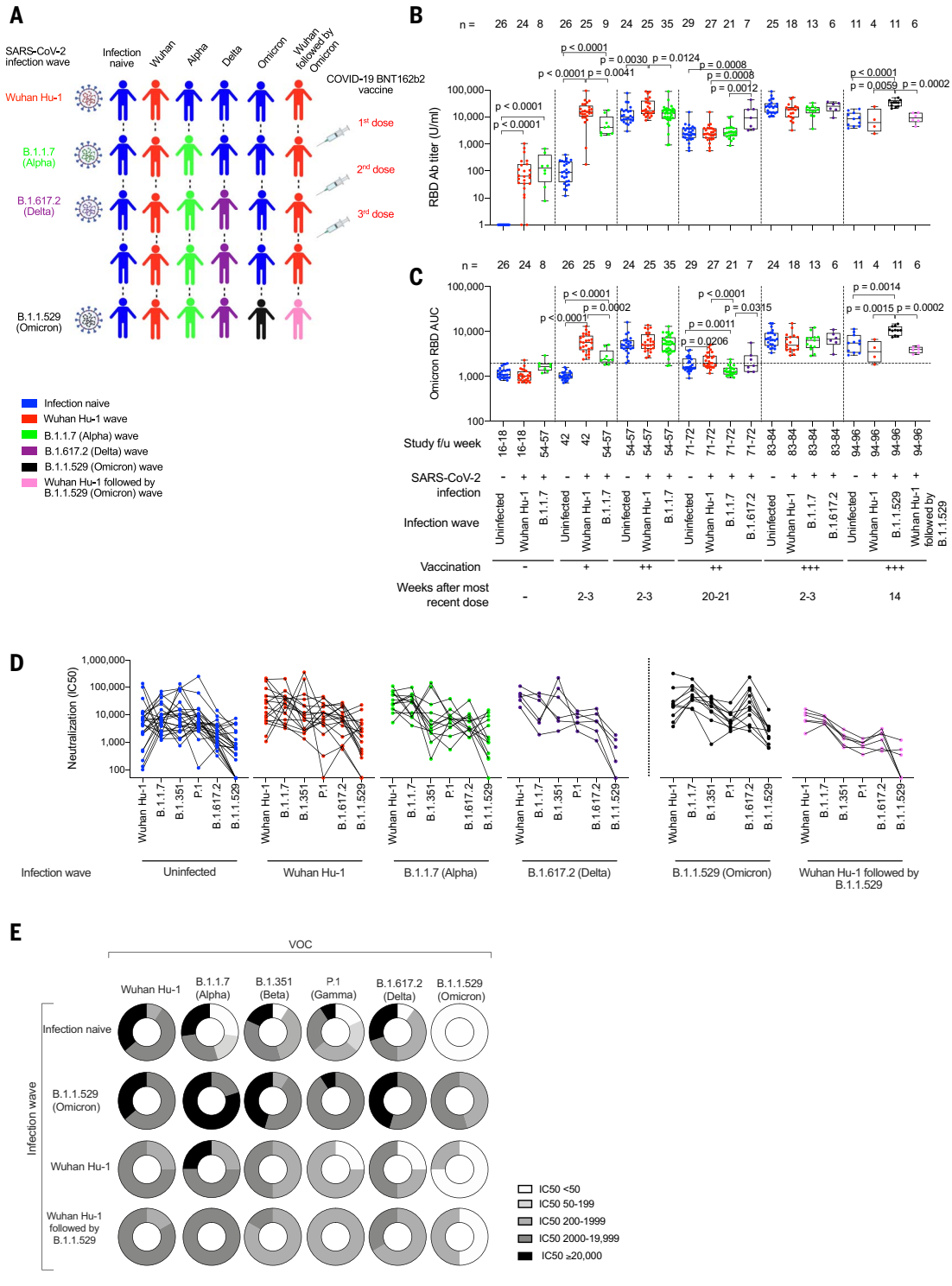

Fig. 6. SARS-CoV-2 infection imprints differential Ab cross-reactivity to VOCs. (**A**) Graphical summary depicting the SARS-CoV-2 infection and vaccination history of HCWs studied. Infection-naïve HCWs are indicated in blue. HCWs infected during the different waves are indicated as follows: ancestral Wuhan Hu-1 (red), B.1.1.7 (Alpha, green) and B.1.617.2 (Delta, purple), B.1.1.529 (Omicron, black), and Wuhan Hu-1 followed by B.1.1.529 (Omicron, pink). (**B** and **C**) Serum Ab binding against ancestral Wuhan Hu-1 S1 RBD (B) and B.1.1.529 (Omicron) S1 RBD (C) in infection-naïve HCWs (blue, n = 11 to 29) or in HCWs with laboratory-confirmed SARS-CoV-2 infection during the ancestral Wuhan Hu-1 (red, n = 4 to 27), B.1.1.7 (Alpha, green, n = 8 to 35), B.1.617.2 (Delta, purple, n = 6 to 7), B.1.1.529 (Omicron, black, n = 11), or Wuhan Hu-1 followed by B.1.1.529 (Omicron, pink, n = 6) waves. Data are shown pre-vaccination and at time points after first, second, and third dose of vaccine. (**D**) Cross-reactive nAb IC_{50} against ancestral Wuhan Hu-1, B.1.1.7 (Alpha), B.1.351 (Beta), P.1 (Gamma), B.1.617.2 (Delta), and B.1.1.529 (Omicron) live virus 2 to 3 weeks after third vaccine dose in infection-naïve HCWs (blue, n = 24) or HCWs with laboratory-confirmed SARS-CoV-2 infection during the Wuhan Hu-1 (red, n = 18), B.1.1.7 (Alpha, green, n = 13), or B.1.617.2 (Delta, purple, n = 6) waves and at 14 weeks (median, 14 weeks; IQR, 3 weeks) after third vaccine dose in HCWs with laboratory-confirmed SARS-CoV-2 during the B.1.1.529 (Omicron, black, n = 11) or Wuhan Hu-1 followed by B.1.1.529 (Omicron, pink, n = 6) waves. Data are plotted pair-wise for individual HCWs. (**E**) Doughnuts showing the relative proportion of HCWs with nAb IC_{50} of <50 (white), 50 to 199 (25% gray), 200 to 1999 (50% gray), 2000 to 19,999 (75% gray), and ≥20,000 (black) against ancestral Wuhan Hu-1, B.1.1.7 (Alpha), B.1.351 (Beta), P.1 (Gamma), B.1.617.2 (Delta), and B.1.1.529 (Omicron) live virus in infection-naïve HCWs (n = 11) or HCWs with laboratory confirmed infection during the B.1.1.529 (Omicron, n = 11), Wuhan Hu-1 (n = 4), or Wuhan Hu-1 followed by B.1.1.529 (Omicron, n = 6) waves at 14 weeks (median, 14 weeks; IQR, 3 weeks) after the third vaccine dose. Statistical tests were performed using Prism 9.0. [(B) and (C)] Mann-Whitney U test.

previously Wuhan Hu-1 or B.1.1.7 (Alpha) infected HCWs made similar responses (Fig. 6, B and C).

However, 20 to 21 weeks after the second vaccine dose, differential B.1.1.529 (Omicron) RBD Ab waning was noted, with almost all (19/21) HCWs infected during the second B.1.1.7 (Alpha) wave no longer showing detectable cross-reactive antibody against B.1.1.529 (Omicron) RBD (Fig. 6C). This was distinct from HCWs infected by Wuhan Hu-1 during the first wave, who demonstrated a significantly higher cross-protective antibody response against B.1.1.529 (Omicron) RBD ($P < 0.0001$) (Fig. 6C). This indicates a profound differential impact of immune imprinting on B.1.1.529 (Omicron)–specific immune antibody waning between HCWs infected by Wuhan Hu-1 and B.1.1.7 (Alpha), as this differential is not seen in Ab responses to ancestral Wuhan Hu-1 spike S1 RBD (Fig. 6B).

Again, there was a leveling up back to similar B.1.1.529 (Omicron) RBD binding across infection-naïve and previously infected HCWs [Wuhan Hu-1, B.1.1.7 (Alpha), and B.1.617.2 (Delta)] 2 to 3 weeks after the third vaccine dose (Fig. 6, B and C). Fourteen weeks after the third vaccine dose, previously infection-naïve HCWs infected during the B.1.1.529 (Omicron) wave showed increased S1 RBD B.1.1.529 (Omicron) binding responses, but previously Wuhan Hu-1 infected HCWs did not, indicating that previously Wuhan Hu-1 infected individuals were immune imprinted to not boost antibody binding responses against B.1.1.529 (Omicron) despite having been infected by B.1.1.529 (Omicron) itself (Fig. 6C).

In fact, infection during the B.1.1.529 (Omicron) wave imprinted a consistent relative hierarchy of cross-neutralization immunity against VOCs across different individuals with potent cross-reactive nAb responses against B.1.1.7 (Alpha), B.1.351 (Beta), and B.1.617.2 (Delta) (Fig. 6, D and E). Comparative analysis of nAb potency for cross-neutralization of VOCs emphasized the impact of immune imprinting which effectively abrogates the nAb responses in those vaccinated HCWs infected during the first wave and then reinfected during the B.1.1.529 (Omicron) wave. The doughnuts in Fig. 6E highlight the extent to which the relative potency of nAb responses are attenuated in previously Wuhan Hu-1 infected HCWs.

Discussion

At this stage in the pandemic, there is a view that the global spread of B.1.1.529 (Omicron), through its association with a relatively milder disease phenotype and, possibly, a potential to boost vaccine immunity, may herald the transition into a new, endemic relationship (*28*). The case for vaccine-mediated immune preconditioning as key mediator of the attenuated phenotype is complex: Although functional neutralization by vaccine-primed sera is considerably blunted against B.1.1.529 (Omicron), three-dose vaccination efficacy against symptomatic disease holds up, in the 50 to 70% range (*6*–*8*). It has thus been proposed that immune protection may be supported by maintenance of relatively high T cell response frequencies to viral epitopes unperturbed by loss of antibody epitopes (*13*–*18*). A rationale for this T cell–mediated protection comes from animal studies showing the direct ability of SARS-CoV-2–specific T cells to curtail lung viral loads (*29*). This raised two key questions with respect to understanding and management of this wave: (i) Considering the very diverse patterns of antiviral immunity shown by ourselves and others to be determined by differential immune imprinting, how would differences in antigen exposure through infection and vaccination alter immune responses against B.1.1.529 (Omicron) at the level of binding antibody and nAb, MBC, and T cell responses? (ii) Is the immune response after infection during the B.1.1.529 (Omicron) wave primed and fully available to support protective immunity? We examined immunity to B.1.1.529 (Omicron) in a longitudinal HCW cohort, considering cross-reactive immunity primed by the varied spike exposures of three-dose vaccination with or without hybrid immunity from any of the Wuhan Hu-1, B.1.1.7 (Alpha), or B.1.617.2 (Delta) infection waves, and then the additive effect of actual infection during the B.1.1.529 (Omicron) wave. In the first part of this paper, we report patterns of response in differentially imprinted, triple-vaccinated HCWs. In the second part, we consider immune responses in those who went on to suffer infection during the B.1.1.529 (Omicron) wave despite triple-vaccination. There were several unexpected findings. Although it is known that cross-reactive antibody recognition is compromised by the mutations in B.1.1.529 (Omicron), it was surprising that this was so profoundly exacerbated by differential imprinting in those who were previously infected by either Wuhan Hu-1 or B.1.1.7 (Alpha). This adds an important dimension to global control of B.1.1.529 (Omicron) in light of the impact B.1.1.7 (Alpha) has had on the global pandemic—by May 2021, B.1.1.7 (Alpha) accounted for 67% of all cases across 149 countries (*30*). That previous SARS-CoV-2 infection history can imprint such a profound, negative impact on subsequent protective immunity is an unexpected consequence of COVID-19. While the notion that, generally, hybrid priming by infection and vaccination enhances immunity is widely agreed upon (*22*), imprinted patterns such as the specific combination of vaccination with infection during the first ancestral Wuhan Hu-1 wave followed by the B.1.1.529 (Omicron) wave require an additional term: "hybrid immune damping." Molecular characterization of the precise mechanism underpinning repertoire shaping from a combination of Wuhan Hu-1 or B.1.1.7 (Alpha) infection and triple-vaccination using ancestral Wuhan Hu-1 sequence, affecting immune responses to subsequent VOCs, will require detailed analysis of differential immune repertoires and their structural consequences. The impact of differential imprinting was seen just as profoundly in T cell recognition of B.1.1.529 (Omicron) S1, which was not recognized by T cells from any triple-vaccinated HCWs who were initially infected during the Wuhan Hu-1 wave and then reinfected during the B.1.1.529 (Omicron) wave. Notably, although B1.1.529 (Omicron) infection in triple-vaccinated previously uninfected individuals could indeed boost antibody, T cell, and MBC responses against other VOCs, responses to Omicron itself were reduced. This relatively poor immunogenicity against itself may help to explain why frequent B.1.1.529 (Omicron) reinfections with short time intervals between infections are proving a novel feature in this wave. It also concurs with observations that mRNA vaccination carrying the B.1.1.529 (Omicron) spike sequence (Omicron third-dose after ancestral sequence prime and boost) offers no protective advantage (*31*). Initial studies using acute serum samples after B.1.1.529 (Omicron) infection had indicated poor immunogenicity and a tendency to elicit only Omicron-specific responses in the unvaccinated and broader responses in those imprinted after COVID-19 vaccination (*32*, *33*), including unexpected patterns of combinations that appeared to ablate neutralizing responses to previously seen VOCs (*33*).

Our T cell analysis, which depended on processing of immunodominant epitopes from whole antigen, revealed a more profound deficit than others. Studies in which T cell responses of vaccinees against spike peptide megapools are screened show that, while there may be a 20% drop in response due to lost epitopes across the entire sequence, most of the response is maintained (*13*–*15*, *17*), albeit with a significant minority showing a completely ablated CD8 response to Omicron peptide pools (*17*). Other studies show that around a fifth of responders to peptide panels have a 50 to 70% drop in T cell response (*16*). Our approach was to evaluate T cell recognition using the dual approach of mapped epitope pools spanning the mutated regions and also whole, naturally processed antigen. We found the greatest impairment of T cell recognition when looking at epitope recognition after processing of whole antigen. Naturally processed epitopes from uptake of whole antigen would generally be considered more representative of the real-life situation and nearer to HLA-ligandome studies than synthetic megapools of several hundred overlapping peptides, which have the potential to drown out physiological response patterns

under the noise of responses from cryptic epitopes that may not feature in real-life natural responses. That is, megapool approaches can, by their nature, underestimate the extent of response ablation. The natural HLA-ligandome of peptides shown to be elicited by natural processing and HLAII presentation only partially overlaps epitopes mapped from overlapping synthetic peptide panels (*34*, *35*). Our immunization of mice with B.1.1.529 (Omicron) mutant epitopes confirmed that de novo T cell response repertoire can be elicited, but this is not necessarily the same as that generated during live infection.

The studies presented here have shown that the high global prevalence of B.1.1.529 (Omicron) infections and reinfections likely reflects considerable subversion of immune recognition at both the B and T cell, antibody binding, and nAb level, although with considerable differential modulation through immune imprinting. Some imprinted combinations, such as infection during the Wuhan Hu-1 and Omicron waves, confer particularly impaired responses.

Materials and methods

Study subjects

A total of 731 adult HCWs were recruited into the COVIDsortium bioresource in March 2020 (*19*–*24*) (fig. S1). A cross-sectional case-controlled substudy of 136 HCWs recruited 16 to 18 weeks after the March 2020 UK lockdown reported immunity to SARS-CoV-2 infection during the first UK wave (Wuhan Hu-1) (*19*). SARS-CoV-2 infection was determined by baseline, and weekly nasal RNA stabilizing swabs and Roche cobas SARS-CoV-2 reverse transcriptase polymerase chain reaction (RT-PCR) test and baseline and weekly Antibody testing for S1 using the IgG EUROIMMUN enzyme-linked immunosorbent assay (ELISA) and nucleocapsid using the ROCHE Elecsys electrochemiluminescence immunoassay (ECLIA). Antibody ratios >1.1 were deemed positive for the EUROIMMUN SARS-CoV-2 ELISA, and >1 was considered test positive for the ROCHE Elecsys anti-SARS-CoV-2 ECLIA, as evaluated by UK Health Security Agency (UKHSA), Porton Down, UK. A cross-sectional, case-controlled vaccine substudy cohort of 51 HCWs at a mean time point of 22 days (±2 days SD) after administration of the first dose of BNT162b2 vaccines reported immunity to vaccination in individuals with and without a history of prior SARS-CoV-2 infection during the Wuhan Hu-1 wave (*23*). The vaccine substudy recruited HCWs previously enrolled in the 16- to 18-week substudy. It included 25 HCWs (mean age: 44 years; 60% male) with previous lab-defined SARS-CoV-2 infection and 26 HCWs (mean age: 41 years; 54% male) with no laboratory evidence of SARS-CoV-2 infection throughout the initial 16-week longitudinal follow-up. HCWs were followed up longitudinally (n = 51) at a median time point of 20 days [7, interquartile range (IQR)] after administration of the second dose of BNT162b2 (*24*). An additional 358 HCWs were recruited at 55 to 57 weeks follow-up, 53 of whom were infected by the B.1.1.7 (Alpha) VOC during the second UK wave (*24*). At 71 to 72 weeks follow-up, 80 two-dose vaccinated HCWs were re-recruited who were either SARS-CoV-2 infection naïve (n = 27) or had been infected by Wuhan Hu-1 during the first wave (n = 31) or B.1.1.7 (Alpha) during the second UK wave (n = 22) (*24*). At 83 to 84 weeks, 62 HCWs had been recruited who were either SARS-CoV-2 infection–naïve (n = 25) or had been infected during the first Wuhan Hu-1 (n = 18), second B.1.1.7 (Alpha, n = 13), or third B.1.617.2 (Delta, n = 6) UK infection waves (table S1). All 62 had received a third dose of BNT162b2 at a median time point of 18 days (12, IQR) previously. Thirty-two HCWs were recruited at 94 to 96 weeks, median 14 weeks (3 weeks, IQR) after third-dose vaccination after the onset of the UK B.1.1.529 (Omicron) wave (table S6). This comprised 17 HCWs with PCR-confirmed infection during the Omicron wave. Eleven of these were previously infection-naïve, and six had prior Wuhan Hu-1 infection. A contemporaneous control group of HCWs not infected during the Omicron wave was also recruited; this comprised 11 infection-naïve HCWs and four with prior Wuhan Hu-1 infection. Lack of infection was confirmed by longitudinal N serology status (table S7).

Isolation of PBMCs

Peripheral blood mononuclear cells (PBMCs) were isolated from heparinized blood using Histopaque-1077 Hybri-Max^{T} (Sigma-Aldrich) density gradient centrifugation in SepMate tubes (Stemcell), as previously described (*20*, *23*, *24*). Isolated PBMCs were cryopreserved in fetal bovine serum (FBS) containing 10% dimethyl sulfoxide and stored in liquid nitrogen.

Isolation of serum

Whole blood samples in SST vacutainers (VACUETTE #455092) were clotted at room temperature for at least 1 hour and then centrifuged for 10 min at 800*g*. Serum was aliquoted and stored at −80°C for SARS-CoV-2 antibody detection.

Anti-N and anti-S1 serology

Anti-nucleocapsid and anti-spike antibody detection testing was conducted at UK Health Security Agency using the Roche cobas e801 analyzer. Anti-nucleocapsid antibodies were detected using the qualitative Roche Elecsys anti-SARS-CoV-2 ECLIA nucleocapsid assay (Roche ACOV2, product code: 09203079190) while anti-RBD antibodies were detected using the quantitative Roche Elecsys anti-SARS-CoV-2 ECLIA spike assay (Roche ACOV2S, product code: 09289275190). Assays were performed and calibrated as recommended by the manufacturer. Anti-N results are expressed as a cutoff index (COI) value based on the electrochemiluminescence signal of a two-point calibration, with results COI ≥ 1.0 classified as positive. Anti-spike results are expressed as units per milliliter (U/ml), similarly based on a two-point calibration and a reagent-specific master curve, with a quantitative range of 0.4 to 2500 U/ml. Samples with a value of ≥1.0 U/ml are interpreted as positive for spike antibodies, and samples exceeding >250 U/ml are automatically diluted by the analyzer.

Recombinant proteins

Wuhan Hu-1 SARS-CoV-2 S1 spike protein and B.1.617.2 (Delta) SARS-CoV-2 S1 spike protein (T19R, G142D, del156-157, R158G, L425R, T478K, D614G, P681R) (Z03485-1 and Z03612-1, respectively) were purchased from GenScript USA Inc. B.1.1.529 (Omicron) SARS-CoV-2 S1 spike (A67V, H69del, V70del, T95I, G142D, V143del, Y144del, Y145del, N211del, L212I, ins214EPE, G339D, S371L, S373P, S375F, K417N, N440K, G446S, S477N, T478K, E484A, Q493R, G496S, Q498R, N501Y, Y505H, T547K, D614G, H655Y) and RBD (G339D, S371L, S373P, S375F, K417N, N440K, G446S, S477N, T478K, E484A, Q493R, G496S, Q498R, N501Y, Y505H) proteins (REC32006 and REC32007, respectively) were purchased from the Native Antigen Company.

Peptides

Spike mapped epitope pool (MEP) comprises a previously described pool of eighteen 12- to 20mer peptide epitopes (*20*, *23*, *24*) (table S5A). B.1.1.529 (Omicron) and Wuhan Hu-1 peptide pools are comprised of peptides with the B.1.1.529 (Omicron) amino acid mutations and deletions and the respective Wuhan Hu-1 sequences (table S5B). They contain the predicted HLAII binding motifs, as determined by NetMHCIIpan4.0 (*34*) (table S9). Peptides were synthesized by GL Biochem Shanghai Ltd (China).

T cell assay by IFNγ ELISpot

Interferon-γ enzyme-linked immunosorbent spot (IFNγ ELISpot) assays were conducted as previously described (*20*, *23*, *24*). Precoated ELISpot plates (Mabtech 3420-2APT) were washed four times with phosphate-buffered saline (PBS), blocked for 1 hour (at room temperature) with supplemented RPMI1640 (GibcoBRL) [10% heat-inactivated FBS; 1% 100x penicillin, streptomycin and L-glutamine solutions (GibcoBRL)]. Two-hundred thousand PBMCs were seeded per well and stimulated for 18 to 22 hours at 37°C with SARS-CoV-2 recombinant protein [Wuhan Hu-1, B.1.617.2 (Delta), or B.1.1.529 (Omicron) SARS-CoV-2 S1 spike proteins (10 μg/ml)] or peptide pools

(10 μg per ml per peptide). Negative and positive plate controls were medium or anti-CD3 (Mabtech mAb CD3-2). ELISpot plates were developed with 1 μg/ml biotinylated anti-human IFNγ detection Ab conjugated to alk-phosphatase (7-B6-1-ALP, Mabtech), diluted in PBS/0.5% FBS, adding 50 μl per well for 2 hours at room temperature followed by 50 μl per well BCIP/NBT-plus phosphatase substrate (Mabtech), 5 min (at room temperature). Plates were washed and dried before analysis on an AID classic ELISpot plate reader (Autoimmun Diagnostika GMBH, Germany). ELISpot data were analyzed in Microsoft Excel. The average of two culture media only wells was subtracted from all protein/peptide–stimulated wells, and any response that was lower in magnitude than 2 SD of the sample-specific control wells was not considered a stimulation-specific response. Results were expressed as difference in (delta) SFCs per 10^6 PBMCs between negative control and protein/peptide stimulation conditions. Results were excluded if negative control wells showed >100 SFCs per 10^6 PBMCs (n = 4) or cell viability was low, with <1000 SFCs per 10^6 PBMCs in anti-CD3 positive control wells (n = 5). Results were plotted using Prism 9.0 for Mac OS (GraphPad).

B cell ELISpots

Before B cell ELISpot assays, PBMCs were cultured for 5 days (37°C/5% CO_2) in 24-well plates, 500,000 cells per well containing 1 μg/ml TLR7/8 agonist R848 plus 10 ng/ml recombinant human IL-2 (Mabtech Human Memory B cell Stimpack 3660-1). After 4 days, PBMC stimulation ELISpot PVDF plates (Millipore MSIPS4W10) were coated with PBS, purified anti-human IgG MT91/145 (10 μg/ml, Mabtech 3850-3-250), and Wuhan Hu-1, B.1.617.2, or B.1.1.529 SARS-CoV-2 S1 spike proteins (10 μg/ml) and incubated at 4°C overnight. Plates were washed five times and blocked for 1 hour with RPMI1640 [supplemented with 10% heat-inactivated FBS, 1% 100x penicillin, streptomycin, and L-glutamine solutions (GibcoBRL)]. Pre-stimulated PBMCs were washed twice before seeding at 7500 to 15,000 cells per well for anti-human IgG coated wells and 15,000 to 150,000 cells per well for SARS-CoV-2 spike coated wells. Assays were run in duplicate. Plates were incubated at 37°C for 18 to 20 hours. For ELISpot development, plates were washed five times with PBS/0.05% Tween 20 (PBST) before incubation with 100 μl biotinylated anti-human IgG MT78/145 (Mabtech 3850-6-250), in PBS/0.5% FBS for 2 hours at room temperature. Plates were washed five times in PBST and incubated with 100 μl per well 1:1000 Streptavidin-ALP (Mabtech 3310-10-1000), in PBS/0.5% FBS for 1 hour at room temperature. Plates were then washed five times with PBST, and spots were developed by adding 100 μl per well BCIP/NBT substrate (Mabtech). Reactions were stopped by washing in tap water, and plates were dried before being analyzing on an AID classic ELISpot plate reader (Autoimmun Diagnostika GMBH, Germany). Analysis of ELISpot data was performed in Microsoft Excel. Spots counted for each well were adjusted for cell numbers seeded, and the average of PBS-only coated wells was subtracted from antigen-coated wells. The number of SARS-CoV-2 spike antigen–specific Ab secreting cells (ASCs) was expressed as a percent of the total number of IgG ASC.

B.1.1.529 (Omicron) RBD ELISA

Nunc 96-well immune ELISA plates were coated with 1 μg/ml of B.1.1.529 (Omicron) Spike RBD protein in carbonate buffer (Sigma Aldrich) for 2 hours at 37°C before washing with PBS (0.05% Tween) (PBST) and blocking at 37°C for 1 hour with PBS containing 1% bovine serum albumin (BSA). Plates were washed in PBST again before application of 50 μl of diluted sera to each well. All serum dilutions were run in duplicate, and a four-point dilution series was run for each sample. After overnight incubation at 4°C, plates were washed with PBST, and wells were incubated with 1:1000 dilution of Biotin Mouse Anti-human IgG (BD Pharmingen, 555785) at room temperature for 1 hour. Plates were washed again before application of 1:200 dilution of streptavidin horseradish peroxidase (HRP) (Bio-techne, DY998) for 30 min followed by a final wash and then assay development using 3,3′, 5,5;-tetramethylbenzidine (TMB) substrate (Sigma Aldrich, T0440). Color development was stopped after 5 min by the addition of 0.18 M H_2SO_4 and OD450nm values for each well measured using a FLUOstar Omega Plate Reader. Analysis of ELISA data was performed in Prism 9.0 for Mac OS (GraphPad). Data for serial dilutions were plotted, and area under the curve calculated for each individual serum sample.

Multiplex variant-specific IgG antibody measurement

Antibody titers against VOC-specific spike antigens (RBD or spike) were measured using the multiplex MesoScale Discovery (MSD) electrochemiluminescent immunoassay (V-Plex, MSD, Gaithersburg). IgG binding antibody to the RBD domain for the different VOCs were determined using the V-Plex Panel 22 (Catalogue number K15559U), which includes the RBD antigens of "wild-type" SARS-CoV-2, B.1.1.529/BA.1 (Omicron), B.1.1.7 (Alpha), B.1.351/B.1.351.1 (Beta), P.1 (Gamma), and AY.3/AY.4/B.1.617.2 (Delta). IgG binding antibody to the full spike protein of the different VOC were determined using V-Plex Panel 23 (Catalogue numb er K15567U) which includes spike antigens of "wild-type" SARS-CoV-2, AY.4.2 (Delta sublineage), B.1.1.529/BA.1 (Omicron), B.1.1.7 (Alpha), B.1.351 (Beta), P.1 (Gamma), B.1.617.2/AY.3/ AY.5 (Delta and Delta sublineages), and AY.4 (Delta alternative sequence and sublineages) (*36*, *37*). A full list of each antigen and its included mutations can be found in the supplementary materials (table S2).

In brief, plates were run per manufacturer's instructions, with washing between incubations performed using a Biotek 405TS plate washer. Plates were blocked for 30 min with 5% BSA before the addition of samples diluted between 1:1000 and 1:100,000. Samples were incubated for 2 hours, followed by addition of the secondary anti-human IgG antibody (Sulfo-tag) for 1 hour. Read buffer was added to plates before reading immediately using the MSD QuickPlex SQ 120 platform. Only results from antigen spots within the detection range were used for the final analysis. Results were reported as arbitrary units per milliliter (AU/ml) determined against a seven-point calibration curve using serially diluted reference standard 1.

Authentic Wuhan Hu-1 SARS-CoV-2 and VOC variant titration

SARS-CoV-2 isolate stocks [including Wuhan Hu-1, B.1.1.7 (Alpha), B.1.351 (Beta), P.1 (Gamma), B.1.617.2 (Delta), and B.1.1.529 (Omicron)] used in experiments (table S8) were prepared and titrated as previously described (*23*, *24*).

Authentic Wuhan Hu-1 SARS-CoV-2 and VOC microneutralization assays

SARS-CoV-2 microneutralization assays were carried out as described previously (*23*, *24*). VeroE6 cells were seeded in 96-well plates 24 hours before infection. Duplicate titrations of heat-inactivated participant sera were incubated with 3×10^4 focus-forming units of SARS-CoV-2 virus (TCID100) at 37°C for 1 hour. Serum/virus preparations were added to cells and incubated for 72 hours. Surviving cells were fixed in formaldehyde and stained with 0.1% (w/v) crystal violet solution [crystal violet was resolubilized in 1% (w/v) sodium dodecyl sulfate solution]. Absorbance readings were taken at 570 nm using a CLARIOStar Plate Reader (BMG Labtech). Negative controls of pooled pre-pandemic sera (collected before 2008) and pooled serum from neutralization-positive SARS-CoV-2 convalescent individuals were spaced across the plates. Absorbance for each well was standardized against technical positive (virus control) and negative (cells only) controls on each plate to determine percentage neutralization values. IC_{50} values were determined from neutralization curves. All authentic SARS-CoV-2 propagation and microneutralization assays were performed in a containment level 3 facility.

In silico epitope prediction for B.1.1.529 (Omicron) and BA.2

In silico predictions of HLA-DRB1 peptide-binding were performed using NetMHCIIpan-4.0

(*38*) on the basis of a peptide length of 15 amino acids (tables S9 and S13). HLA core binding sequences containing individual mutations were selected if contained within a peptide defined as a strong or weak binder by the NetMHCIIpan-4.0 default parameters of rank score <1% (threshold for strong binder) and rank score <5% (threshold for weak binder). For HLA-A, HLA-B, and HLA-C alleles, analysis was performed using NetMHCpan-4.1 on the basis of peptide lengths of 8, 9, and 10 amino acids (tables S10 to S12 and S14 to S16). Again, the default parameters of rank score ≤ 0.5% (threshold for strong binder) and ≤ 2% (threshold for weak binder) were used.

*HLA-DRB1*0401 transgenic T cell assays*

Studies using HLAII transgenics carrying DRB1*0401 in the context of a homozygous knockout for murine H2-Aβ have been previously described (*39*, *40*). Mice (7 to 8 weeks old) were immunized in one hind footpad with B.1.1.529 (Omicron) variant or Wuhan Hu-1 pools or peptides containing 10 μg of each peptide sequence in Hunters Titermax Gold adjuvant (Sigma Aldrich). Popliteal lymph nodes were collected at d10 and prepared as single-cell suspensions. IFNγ ELISpot assays were performed in triplicate in HL1 serum-free medium (Lonza) [supplemented with 1% 100x L-glutamine and 0.5% 100x penicillin/streptomycin solutions (GibcoBRL)]. PVDF ELISpot plates (Merck Millipore MSIPN4550) were coated with anti-mouse IFNγ capture antibody (Diaclone Murine IFN gamma ELISpot Set, 862.031.020) overnight before seeding 200,000 lymph node cells per well and stimulating (72 hours, 37°C with 5% CO_2) with peptide pools or individual SARS-CoV-2 Wuhan Hu-1 or variant peptides (10 μg per ml per peptide). Internal plate controls were culture media alone and staphylococcal enterotoxin B (SEB). Assays were developed using biotinylated anti-mouse IFNγ followed by streptavidin-alkaline phosphatase conjugate and BCIP/NTB substrate (Diaclone) before washing in tap water, drying, and analyzing using an AID classic ELISpot plate reader (Autoimmun Diagnostika GMBH, Germany). Analysis of ELISpot data was performed in Microsoft Excel. The average from three culture media wells was subtracted from peptide-stimulated wells, and any response that was <2 SD of the sample-specific control wells was not considered a peptide-specific response. Results were expressed as difference in (delta) SFCs per 10^6 PBMCs between the negative control and peptide stimulation conditions. Results were plotted using Prism 9.0 for Mac OS (GraphPad).

For transcriptomic analysis, lymph node cells were cultured with no peptide or with 10 μg/ml Wuhan Hu-1 or B.1.1.529 (Omicron) variant G142/del143-5 or Q493R/G496S/Q498R/N501Y/Y505H peptides. At 24 hours, cells were harvested and lysed for RNA extraction. RNA was extracted using an Agilent RNA microprep kit. cDNA was prepared using an RT2 first strand kit (Qiagen), and qPCR for target genes was performed using RT^2 profiler PCR array Mouse T Helper Cell Differentiation plates (Qiagen PAMM-503Z). Data were analyzed and plotted using the Qiagen GeneGlobe data analysis tool and genes up-regulated by peptide stimulation with $P > 0.05$ (by Student's *t* test) compared with no peptide stimulation were identified.

Statistics and reproducibility

Data were assumed to have a non-Gaussian distribution. Wilcoxon matched-pairs signed rank test and a Mann-Whitney *U* test were used for single, paired, and unpaired comparisons. Nonparametric tests were used throughout. $P < 0.05$ was considered significant. Prism 9.0 for Mac was used for analysis.

REFERENCES AND NOTES

1. S. S. A. Karim, Q. A. Karim, Omicron SARS-CoV-2 variant: A new chapter in the COVID-19 pandemic. *Lancet* **398**, 2126–2128 (2021). doi: 10.1016/S0140-6736(21)02758-6; pmid: 34871545
2. P. Elliott *et al*., Rapid increase in Omicron infections in England during December 2021: REACT-1 study. *Science* **375**, 1406–1411 (2022). doi: 10.1126/science.abn8347; pmid: 35133177
3. S. A. Madhi *et al*., Population immunity and Covid-19 severity with omicron variant in South Africa. *N. Engl. J. Med.* **386**, 1314–1326 (2022). doi: 10.1056/NEJMoa2119658; pmid: 35196424
4. K. P. Y. Hui *et al*., SARS-CoV-2 Omicron variant replication in human bronchus and lung ex vivo. *Nature* **603**, 715–720 (2022). doi: 10.1038/s41586-022-04479-6; pmid: 35104836
5. A. Sigal, Milder disease with Omicron: Is it the virus or the pre-existing immunity? *Nat. Rev. Immunol.* **22**, 69–71 (2022). doi: 10.1038/s41577-022-00678-4; pmid: 35046570
6. S. Collie, J. Champion, H. Moultrie, L.-G. Bekker, G. Gray, Effectiveness of BNT162b2 vaccine against omicron variant in South Africa. *N. Engl. J. Med.* **386**, 494–496 (2022). doi: 10.1056/NEJMc2119270; pmid: 34965358
7. H. F. Tseng *et al*., Effectiveness of mRNA-1273 against SARS-CoV-2 Omicron and Delta variants. *Nat. Med.* **28**, 1063–1071 (2022). doi: 10.1038/s41591-022-01753-y; pmid: 35189624
8. N. Andrews *et al*., Covid-19 vaccine effectiveness against the omicron (B.1.1.529) variant. *N. Engl. J. Med.* **386**, 1532–1546 (2022). doi: 10.1056/NEJMoa2119451; pmid: 35249272
9. D. Planas *et al*., Considerable escape of SARS-CoV-2 Omicron to antibody neutralization. *Nature* **602**, 671–675 (2022). doi: 10.1038/s41586-021-04389-z; pmid: 35016199
10. L. Liu *et al*., Striking antibody evasion manifested by the Omicron variant of SARS-CoV-2. *Nature* **602**, 676–681 (2022). doi: 10.1038/s41586-021-04388-0; pmid: 35016198
11. S. Cele *et al*., Omicron extensively but incompletely escapes Pfizer BNT162b2 neutralization. *Nature* **602**, 654–656 (2022). doi: 10.1038/s41586-021-04387-1; pmid: 35016196
12. A. Muik *et al*., Neutralization of SARS-CoV-2 Omicron by BNT162b2 mRNA vaccine-elicited human sera. *Science* **375**, 678–680 (2022). doi: 10.1126/science.abn7591; pmid: 35040667
13. A. Tarke *et al*., SARS-CoV-2 vaccination induces immunological T cell memory able to cross-recognize variants from Alpha to Omicron. *Cell* **185**, 847–859.e11 (2022). doi: 10.1016/j.cell.2022.01.015; pmid: 35139340
14. Y. Gao *et al*., Ancestral SARS-CoV-2-specific T cells cross-recognize the Omicron variant. *Nat. Med.* **28**, 472–476 (2022). doi: 10.1038/s41591-022-01700-x; pmid: 35042228
15. J. Liu *et al*., Vaccines elicit highly conserved cellular immunity to SARS-CoV-2 Omicron. *Nature* **603**, 493–496 (2022). doi: 10.1038/s41586-022-04465-y; pmid: 35102312
16. V. Naranbhai *et al*., T cell reactivity to the SARS-CoV-2 Omicron variant is preserved in most but not all individuals. *Cell* **185**, 1041–1051.e6 (2022). pmid: 35202566
17. R. Keeton *et al*., T cell responses to SARS-CoV-2 spike cross-recognize Omicron. *Nature* **603**, 488–492 (2022). doi: 10.1038/s41586-022-04460-3; pmid: 35102311
18. R. R. Goel *et al*., Efficient recall of Omicron-reactive B cell memory after a third dose of SARS-CoV-2 mRNA vaccine. *Cell* **185**, 1875–1887.e8 (2022). doi: 10.1016/j.cell.2022.04.009; pmid: 35523182
19. T. A. Treibel *et al*., COVID-19: PCR screening of asymptomatic health-care workers at London hospital. *Lancet* **395**, 1608–1610 (2020). doi: 10.1016/S0140-6736(20)31100-4; pmid: 32401714
20. C. J. Reynolds *et al*., Discordant neutralizing antibody and T cell responses in asymptomatic and mild SARS-CoV-2 infection. *Sci. Immunol.* **5**, eabf3698 (2020). doi: 10.1126/sciimmunol.abf3698; pmid: 33361161
21. C. Manisty *et al*., Time series analysis and mechanistic modelling of heterogeneity and sero-reversion in antibody responses to mild SARS-CoV-2 infection. *EBioMedicine* **65**, 103259 (2021). doi: 10.1016/j.ebiom.2021.103259; pmid: 33662833
22. C. Manisty *et al*., Antibody response to first BNT162b2 dose in previously SARS-CoV-2-infected individuals. *Lancet* **397**, 1057–1058 (2021). doi: 10.1016/S0140-6736(21)00501-8; pmid: 33640038
23. C. J. Reynolds *et al*., Prior SARS-CoV-2 infection rescues B and T cell responses to variants after first vaccine dose. *Science* **372**, 1418–1423 (2021). doi: 10.1126/science.abh1282; pmid: 33931567
24. C. J. Reynolds *et al*., Heterologous infection and vaccination shapes immunity against SARS-CoV-2 variants. *Science* **375**, 183–192 (2022). doi: 10.1126/science.abm0811; pmid: 34855510
25. UK Office for National Statistics, Coronavirus (COVID-19) latest insights: Infections; https://www.ons.gov.uk/peoplepopulationandcommunity/healthandsocialcare/conditionsanddiseases/articles/coronaviruscovid19latestinsights/infections.
26. M. McCallum *et al*., N-terminal domain antigenic mapping reveals a site of vulnerability for SARS-CoV-2. *Cell* **184**, 2332–2347.e16 (2021). doi: 10.1016/j.cell.2021.03.028; pmid: 33761326
27. G. Cerutti *et al*., Potent SARS-CoV-2 neutralizing antibodies directed against spike N-terminal domain target a single supersite. *Cell Host Microbe* **29**, 819–833.e7 (2021). doi: 10.1016/j.chom.2021.03.005; pmid: 33789084
28. E. Callaway, Beyond Omicron: What's next for COVID's viral evolution. *Nature* **600**, 204–207 (2021). doi: 10.1038/d41586-021-03619-8; pmid: 34876665
29. B. Israelow *et al*., Adaptive immune determinants of viral clearance and protection in mouse models of SARS-CoV-2. *Sci. Immunol.* **6**, eabl4509 (2021). doi: 10.1126/sciimmunol.abl4509; pmid: 34623900
30. GISAID, Tracking of Variants; https://www.gisaid.org/hcov19-variants/.
31. M. Gagne *et al*., mRNA-1273 or mRNA-Omicron boost in vaccinated macaques elicits similar B cell expansion, neutralizing responses, and protection from Omicron. *Cell* **185**, 1556–1571.e18 (2022). doi: 10.1016/j.cell.2022.03.038; pmid: 35447072
32. S. I. Richardson *et al*., SARS-CoV-2 Omicron triggers cross-reactive neutralization and Fc effector functions in previously vaccinated, but not unvaccinated, individuals. *Cell Host Microbe* **30**, 880–886.e4 (2022). doi: 10.1016/j.chom.2022.03.029; pmid: 35436444
33. A. Rössler, L. Knabl, D. von Laer, J. Kimpel, Neutralization profile after recovery from SARS-CoV-2 omicron infection. *N. Engl. J. Med.* **386**, 1764–1766 (2022). doi: 10.1056/NEJMc2201607; pmid: 35320661
34. M. D. Knierman *et al*., The human leukocyte antigen class II immunopeptidome of the SARS-CoV-2 spike glycoprotein. *Cell Rep.* **33**, 108454 (2020). doi: 10.1016/j.celrep.2020.108454; pmid: 33220791
35. R. Parker *et al*., Mapping the SARS-CoV-2 spike glycoprotein-derived peptidome presented by HLA class II on dendritic cells. *Cell Rep.* **35**, 109179 (2021). doi: 10.1016/j.celrep.2021.109179; pmid: 34004174
36. Meso Scale Diagnostics, V-PLEX SARS-CoV-2 Panel 22 (IgG) Kit; https://www.mesoscale.com/products/v-plex-sars-cov-2-panel-22-igg-kit-k15559u/.
37. Meso Scale Diagnostics, V-PLEX SARS-CoV-2 Panel 23 (IgG) Kit; https://www.mesoscale.com/products/v-plex-sars-cov-2-panel-23-igg-kit-5-pl-k15567u/.
38. B. Reynisson, B. Alvarez, S. Paul, B. Peters, M. Nielsen, NetMHCpan-4.1 and NetMHCIIpan-4.0: Improved predictions of

MHC antigen presentation by concurrent motif deconvolution and integration of MS MHC eluted ligand data. *Nucleic Acids Res.* **48**, W449–W454 (2020). doi: 10.1093/nar/gkaa379; pmid: 32406916
39. K. J. Quigley *et al*., Chronic infection by mucoid *Pseudomonas aeruginosa* associated with dysregulation in T-cell immunity to outer membrane porin F. *Am. J. Respir. Crit. Care Med.* **191**, 1250–1264 (2015). doi: 10.1164/rccm.201411-19950C; pmid: 25789411
40. C. Reynolds *et al*., T cell immunity to the alkyl hydroperoxide reductase of *Burkholderia pseudomallei*: A correlate of disease outcome in acute melioidosis. *J. Immunol.* **194**, 4814–4824 (2015). doi: 10.4049/jimmunol.1402862; pmid: 25862821

ACKNOWLEDGMENTS

The authors thank HCW participants for participating in the study and the research teams involved in recruitment, obtaining consent, and sampling the HCW participants. The SARS-CoV-2 Wuhan Hu-1 Human 2019-nCoV Isolate EVA catalog code 026V-03883 was obtained from European Virus Archive Global (EVAg), Charité – Universitätsmedizin Berlin. The SARS-CoV-2 B.1.1.7 isolate was obtained from the National Institute for Biological Standards and Control (NIBSC), thanks to the contribution of PHE Porton Down and S. Funnell. The nCoV19 isolate/UK ex South African/2021 lineage B.1.351 EVA catalog code 04V-04071 was obtained from EVAg, PHE Porton Down. P.1, B.1.617.2, and B.1.1.529. isolates were purchased from EVAg. Figures 1A, 4A, and 6A in this manuscript were created with BioRender.com. **Funding:** R.J.B. and D.M.A. are supported by MRC (MR/S019553/1, MR/R02622X/1, MR/V036939/1, and MR/W020610/1), NIHR Imperial Biomedical Research Centre (BRC):ITMAT, Cystic Fibrosis Trust SRC (2019SRC015), NIHR EME Fast Track (NIHR134607), NIHR Long Covid (COV-LT2-0027), Innovate UK (SBRI 10008614), and Horizon 2020 Marie Skłodowska-Curie Innovative Training Network (ITN) European Training Network (860325). Á.M. is supported by MRC (MR/W020610/1), NIHR EME Fast Track (NIHR134607), Rosetrees Trust, the John Black Charitable Foundation, and Medical College of St Bartholomew's Hospital Trust. The COVIDsortium is supported by funding donated by individuals, charitable trusts, and corporations including Goldman Sachs, Kenneth C Griffin, the Guy Foundation, GW Pharmaceuticals, Kusuma Trust, and Jagclif Charitable Trust and enabled by Barts Charity with support from UCLH Charity. Wider support is acknowledged on the COVIDsortium website (https://covid-consortium.com/). Institutional support from Barts Health NHS Trust and Royal Free NHS Foundation Trust facilitated study processes, in partnership with University College London and Queen Mary University of London. J.C.M., C.M., and T.A.T. are directly and indirectly supported by the University College London Hospitals (UCLH) and Barts NIHR Biomedical Research Centres and through the British Heart Foundation (BHF) Accelerator Award (AA/18/6/34223). T.A.T. is funded by a BHF Intermediate Research Fellowship (FS/19/35/34374). The funders had no role in study design, data collection, data analysis, data interpretation, or writing of the report. **Ethics statement:** The COVIDsortium HCW bioresource is registered on ClinicalTrials.gov (NCT04318314) and approved by the UK National Research Ethics Service (20/SC/0149). Subjects gave written, informed consent, and the study conformed to the Helsinki Declaration principles. Mouse experiments were performed under UK Home Office Legislation and the Animals (Scientific Procedures) Act 1986 and Project License P809B6A94 granted for this work. **Author contributions:** R.J.B. conceptualized, designed, and led the study reported here. R.J.B. and D.M.A. designed and supervised T cell and B cell experiments and HLAII transgenic experiments. Á.M. designed and supervised the nAb experiments. T.B. and A.S. supervised whole spike and S1 RBD IgG and N IgG/IgM studies. C.J.R. developed, performed, and analyzed T cell and memory B cell experiments and HLAII transgenic and transcriptomic experiments. J.M.G. and C.P. developed, performed, and analyzed nAb experiments. A.D.O. performed and A.Se. analyzed whole spike, RBD, and N antibody assays. T.B., C.M., Á.M., T.A.T., J.C.M., and M.N. conceptualized and established the COVIDsortium HCW cohort. R.J.B, T.A.T., J.C.M., and C.M. conceptualized and designed the vaccine substudy cohort. G.J., N.F., C.M., T.A.T., and J.C.M. recruited HCWs and collected samples. C.J.R., D.M.S., K.-M.L., F.P.P., S.L., and D.K.B. processed HCW samples. C.J.R., J.M.G., C.P., Á.M., A.D.O., D.M.A., and R.J.B. analyzed the data. C.J.R., J.M.G., C.P., A.D.O., C.M., T.A.T., J.C.M., A.S., T.B., Á.M., D.M.A., and R.J.B. interpreted the data. R.J.B. and D.M.A. wrote the original and revised manuscripts with input from the authors. All authors reviewed and approved the manuscript and figures. **Competing interests:** R.J.B. and D.M.A. are members of the Global T cell Expert Consortium and have consulted for Oxford Immunotec outside the submitted work. **Data and materials availability:** All data needed to evaluate the conclusions in the paper are present in the paper or the supplementary materials. The SARS-CoV-2 Wuhan Hu-1 Human 2019-nCoV, B.1.351, P.1, B.1.617.2, and B.1.1.529 isolates were obtained under material agreements with EVAg, France. The SARS-CoV-2 B.1.1.7 isolate was obtained under a material agreement with NIBSC, UK.

SUPPLEMENTARY MATERIALS

science.org/doi/10.1126/science.abq1841
Figs. S1 to S6
Tables S1 to S17
COVIDsortium Investigators
COVIDsortium Immune Correlates Network
MDAR Reproducibility Checklist

View/request a protocol for this paper from *Bio-protocol*.

Submitted 23 March 2022; accepted 6 June 2022
10.1126/science.abq1841

Science

Immune boosting by B.1.1.529 (Omicron) depends on previous SARS-CoV-2 exposure

Catherine J. ReynoldsCorinna PadeJoseph M. GibbonsAshley D. OtterKai-Min LinDiana Muñoz SandovalFranziska P. PieperDavid K. ButlerSiyi LiuGeorge JoyNasim ForooghiThomas A. TreibelCharlotte ManistyJames C. MoonAmanda SemperTim BrooksÁine McKnightDaniel M. AltmannRosemary J. Boyton, and Hakam Abbass, and Aderonke Abiodun, and Mashael Alfarih, and Zoe Alldis, and Daniel M. Altmann, and Oliver E. Amin, and Mervyn Andiapen, and Jessica Artico, and João B. Augusto, and Georgina L. Baca, and Sasha N. L. Bailey, and Anish N. Bhuva, and Alex Boulter, and Ruth Bowles, and Rosemary J. Boyton, and Olivia V. Bracken, and Ben O'Brien, and Tim Brooks, and Natalie Bullock, and David K. Butler, and Gabriella Captur, and Olivia Carr, and Nicola Champion, and Carmen Chan, and Aneesh Chandran, and Tom Coleman, and Jorge Couto de Sousa, and Xose Couto-Parada, and Eleanor Cross, and Teresa Cutino-Moguel, and Silvia D'Arcangelo, and Rhodri H. Davies, and Brooke Douglas, and Cecilia Di Genova, and Keenan Dieobi-Anene, and Mariana O. Diniz, and Anaya Ellis, and Karen Feehan, and Malcolm Finlay, and Marianna Fontana, and Nasim Forooghi, and Sasha Francis, and Joseph M. Gibbons, and David Gillespie, and Derek Gilroy, and Matt Hamblin, and Gabrielle Harker, and Georgia Hemingway, and Jacqueline Hewson, and Wendy Heywood, and Lauren M. Hickling, and Bethany Hicks, and Aroon D. Hingorani, and Lee Howes, and Ivie Itua, and Victor Jardim, and Wing-Yiu Jason Lee, and Melaniepetra Jensen, and Jessica Jones, and Meleri Jones, and George Joy, and Vikas Kapil, and Caoimhe Kelly, and Hibba Kurdi, and Jonathan Lambourne, and Kai-Min Lin, and Siyi Liu, and Aaron Lloyd, and Sarah Louth, and Mala K. Maini, and Vineela Mandadapu, and Charlotte Manisty, and Áine McKnight, and Katia Menacho, and Celina Mfuko, and Kevin Mills, and Sebastian Millward, and Oliver Mitchelmore, and Christopher Moon, and James Moon, and Diana Muñoz Sandoval, and Sam M. Murray, and Mahdad Noursadeghi, and Ashley Otter, and Corinna Pade, and Susana Palma, and Ruth Parker, and Kush Patel, and Mihaela Pawarova, and Steffen E. Petersen, and Brian Piniera, and Franziska P. Pieper, and Lisa Rannigan, and Alicja Rapala, and Catherine J. Reynolds, and Amy Richards, and Matthew Robathan, and Joshua Rosenheim, and Cathy Rowe, and Matthew Royds, and Jane Sackville West, and Genine Sambile, and Nathalie M. Schmidt, and Hannah Selman, and Amanda Semper, and Andreas Seraphim, and Mihaela Simion, and Angelique Smit, and Michelle Sugimoto, and Leo Swadling, and Stephen Taylor, and Nigel Temperton, and Stephen Thomas, and George D. Thornton, and Thomas A. Treibel, and Art Tucker, and Ann Varghese, and Jessry Veerapen, and Mohit Vijayakumar, and Tim Warner, and Sophie Welch, and Hannah White, and Theresa Wodehouse, and Lucinda Wynne, and Dan Zahedi, and Benjamin Chain, and James C. Moon

Science, 377 (6603), eabq1841. • DOI: 10.1126/science.abq1841

Importance of infection history

A long-term study of healthcare workers in the United Kingdom has allowed their history of infection and vaccination to be traced precisely. Reynolds *et al*. found some unexpected immune-damping effects caused by infection with a heterologous variant to the latest wave of infection by the Omicron/Pango lineage B.1.1.529. The authors found that Omicron infection boosted immune responses to all other variants, but responses to Omicron itself were muted. Infection with the Alpha variant provided weaker boosting for Omicron-specific responses. Furthermore, Omicron infection after previous Wuhan Hu-1 infection failed to boost neutralizing antibody and T cell responses against Omicron, revealing a profound imprinting effect and explaining why frequent reinfections occur. —CA